

1 TIMETREE OF PRIMATES

2

3 **Using Phylogenomic Data to Explore the Effects of**
4 **Relaxed Clocks and Calibration Strategies on**
5 **Divergence Time Estimation: Primates as a Test Case**

6 Mario dos Reis^{1,2}, Gregg F. Gunnell^{3*}, José Barba-Montoya², Alex Wilkins^{3,4}, Ziheng Yang²
7 and Anne D. Yoder⁵.

8 Correspondence to: *m.dosreisbarros@qmul.ac.uk*

9

10 1. School of Biological and Chemical Sciences, Queen Mary University of London,
11 London, E1 4NS, UK.

12 2. Department of Genetics, Evolution and Environment, University College London,
13 Gower Street, London, WC1E 6BT, UK.

14 3. Division of Fossil Primates, Duke Lemur Center, Durham, NC USA.

15 4. Department of Anthropology, The Ohio State University, Columbus, OH USA.

16 5. Department of Biology, Duke University, Durham, NC USA.

17

18 *Deceased; we dedicate this work to his memory and to the lasting value of his work

19

20 *Abstract.*—Primates have long been a test case for the development of phylogenetic
21 methods for divergence time estimation. Despite a large number of studies, however, the
22 timing of origination of crown Primates relative to the K-Pg boundary and the timing of
23 diversification of the main crown groups remain controversial. Here we analysed a
24 dataset of 372 taxa (367 Primates and 5 outgroups, 61 thousand base pairs) that
25 includes nine complete primate genomes (3.4 million base pairs). We systematically
26 explore the effect of different interpretations of fossil calibrations and molecular clock
27 models on primate divergence time estimates. We find that even small differences in the
28 construction of fossil calibrations can have a noticeable impact on estimated divergence
29 times, especially for the oldest nodes in the tree. Notably, choice of molecular rate model
30 (auto-correlated or independently distributed rates) has an especially strong effect on
31 estimated times, with the independent rates model producing considerably more
32 ancient estimates for the deeper nodes in the phylogeny. We implement
33 thermodynamic integration, combined with Gaussian quadrature, in the program
34 MCMCTree, and use it to calculate Bayes factors for clock models. Bayesian model
35 selection indicates that the auto-correlated rates model fits the primate data
36 substantially better, and we conclude that time estimates under this model should be
37 preferred. We show that for eight core nodes in the phylogeny, uncertainty in time
38 estimates is close to the theoretical limit imposed by fossil uncertainties. Thus, these
39 estimates are unlikely to be improved by collecting additional molecular sequence data.
40 All analyses place the origin of Primates close to the K-Pg boundary, either in the
41 Cretaceous or straddling the boundary into the Palaeogene.

42

43 [Primates; phylogenomic analysis; molecular dating; relaxed clock; fossil; Bayesian
44 analysis; Bayes factors]

45 Divergence time estimation is fundamentally important to every field of evolutionary
46 analysis. Reliable estimates of the timing of speciation events across the Tree of Life
47 allow us to correlate these events with both biotic and abiotic phenomena on geological
48 and more recent timescales, thus illuminating those that are most closely associated
49 with periods of rapid diversification (Zhou et al. 2012; Andersen et al. 2015),
50 evolutionary stasis (Alfaro et al. 2009, Liu et al. 2014), or high rates of extinction (Prum
51 et al. 2015; Zhang et al. 2016). Divergence time analysis was first considered feasible
52 with the publication of Zuckerkandl and Pauling's (1965) "molecular clock" hypothesis.
53 Very soon thereafter, however, it became clear that there are myriad violations to a
54 uniform clock, and in subsequent decades, increasingly sophisticated models have been
55 developed for relaxing the assumptions of a strict clock (Thorne et al. 1998; Kishino et
56 al. 2001; Thorne, and Kishino 2002; Drummond et al. 2006; Lepage, et al. 2007; Rannala
57 and Yang 2007, Heat et al. 2012). These models can be loosely divided into two
58 categories: autocorrelated models, wherein rates of evolution in daughter species are
59 statistically distributed around the parental rates (Sanderson 1997; Thorne et al. 1998;
60 Aris-Brosou and Yang 2002), and uncorrelated models, wherein each lineage on the tree
61 is free to assume a fully independent rate (Drummond et al. 2006; Rannala and Yang
62 2007; Paradis 2013).

63

64 A parallel challenge to divergence time analysis can be observed in the development of
65 calibration strategies (Marshall 1990; Yang and Rannala 2006; Benton and Donoghue
66 2007; Marshall 2008; Dornburg et al. 2011). Given that branch lengths on a phylogeny
67 are the product of rate and time, investigators must assume one to infer the other. The
68 most typical method for breaking this impasse is to employ fossil data as calibrations for
69 one or more nodes in a given phylogeny so that the ages of other nodes can be inferred
70 using DNA sequence data. This places an enormous burden on both the correct
71 placement and age assignment of the fossils. If they are misplaced (i.e., assigned to
72 clades where they do not belong) or if their geological ages are misinterpreted,
73 divergence time estimates for the entire tree can be severely compromised (Martin
74 1993). The uncertainty imposed by paleontological ambiguity has not been as widely
75 appreciated as have been the uncertainties introduced by the finite amount of DNA
76 sequence data, which with the "genomics revolution," is becoming steadily less
77 problematic.

78

79 We have reached a state of the art where branch lengths can be estimated with very high
80 precision. The combination of genome-scale data, sophisticated molecular evolutionary
81 models, and ever-increasing computational power has brought us to this point.

82 Advances in DNA sequencing technology are such that virtually every major clade has at
83 least a few species represented by whole-genome sequences, and this trend is rapidly
84 accelerating. Bayesian methods have been developed such that parameter space can be
85 explored during MCMC estimation, and though violations of the molecular clock will
86 continue to present problems, methods for measuring and accommodating rate
87 variation across phylogenies are explicit and generalizable. And finally, the computing
88 power to integrate this information is increasing steadily. But because of the
89 confounding effect of non-independence of rate and time, the expectation of a
90 conventional Bayesian analysis –that infinite data will eventually overcome prior
91 information and provide posterior distributions with certainty– cannot be met (dos Reis
92 and Yang 2013; Zhu et al. 2015).

93

94 Thus, the field at present is focused on developing a better understanding of the effects
95 of relaxed clock model choice, and on the impacts of calibration points, both with regard
96 to abundance and placement in the phylogeny. Furthermore, in addressing these
97 challenges, it is an open question as to whether simulation studies or tests of empirical
98 data will be more informative for our understanding of best practices. With regard to
99 clock model choice, an empirical study of three independent datasets showed that
100 autocorrelated models outperform uncorrelated models, though the same study found a
101 "high sensitivity" to the relaxation model employed (Lepage et al. 2007), while another
102 empirical study found, however, that an independent rates model was superior (Linder
103 et al. 2011). Simulation studies have only recently been employed, finding that even
104 with complete taxon sampling, rate autocorrelation is challenging to detect (Ho et al.
105 2015). This has led to the conclusion that rigorous model selection should be conducted
106 on a case-by-case basis, utilizing a wide range of real data sets, and thus comprising a
107 promising avenue for future research (Ho et al. 2005; Ho and Duchene 2014; Ho et al.
108 2015).

109

110 With regard to fossil calibration strategies, simulation studies (e.g., Duchene et al. 2014)
111 have thus far agreed with previous empirical studies in finding that multiple calibrations
112 are fundamentally important to accurate age estimation (Soltis et al. 2002; Yoder and
113 Yang 2004; Linder et al. 2005; Rutschmann et al. 2007; Marshall 2008). Duchene et al.
114 (2014) noted that calibrations close to the root of the phylogeny are most powerful.
115 They also found that a significant source of error in divergence time estimation relates
116 to misspecification of the clock model, especially when there are few informative
117 calibrations. We cannot stress enough how sensitive posterior time estimates are to
118 fossil information in constructing the time prior (Inoue et al. 2010). For example,
119 different fossil calibration strategies have led to substantially different estimates of
120 divergence times for mammals (dos Reis et al., 2014a) and early animals (dos Reis et al.
121 2015), regardless of how precise the branch length estimates are (Warnock et al. 2015).
122 Thus, the field has reached the stage wherein there is general agreement that the choice
123 of clock model and calibration strategy are fundamentally important to the accuracy of
124 resulting age estimates, and thus, the way forward will clearly involve both empirical
125 and simulation approaches to the problem.

126

127 Here, we hope to contribute to this progress by conducting an exploration of model
128 choice and calibration strategy in a classic empirical system: the Primates. Despite the
129 fact that it is a relatively small and biologically uniform clade, primates have been
130 inordinately and repeatedly the subject of divergence time analysis, with the first
131 studies appearing at the very outset of molecular clock studies (Sarich and Wilson
132 1967), up to phylogenomic studies encompassing a large set of primate species
133 (Perelman et al. 2011; Springer et al. 2012). This is largely due, undoubtedly, to the fact
134 that we ourselves are members of this clade and can thus be forgiven for a persistent
135 curiosity about our ancestral history. Age estimates for major primate divergence
136 events have varied broadly among different studies (see Table 1), though one result has
137 been relatively constant throughout: primate origins have been typically shown to
138 predate the Cretaceous-Paleogene (K-Pg) mass-extinction event.

139

140 Our study explores the effects of an autocorrelated versus an uncorrelated rate model
141 on age estimates, and also explores the consequences of two different interpretations of
142 both the age and the placement of key fossils with the living primate radiation. We

143 apply these two strategies to a large phylogenomic dataset for Primates (372 species
144 with 61 thousand base pairs and 9 species with 3.4 million base pairs). Until very
145 recently, reliable calculations of branch lengths and age estimates within an analysis of
146 this magnitude would have been beyond the capacity of computational methods. We
147 have tackled many of these challenges by deploying the sequential Bayesian procedure
148 used by dos Reis et al. (2012) wherein the posterior age estimates derived from a small
149 taxonomic sample with genome-scale data are then deployed as priors for a subsequent
150 analysis with many species and a much-reduced nucleotide sample. This procedure
151 reduces the computational cost of a typical combined data analysis. It also helps to
152 alleviate the concerns with the "missing data" problem, because in the sequential
153 analysis the analysis of times on the genome-scale partition are carried out on a 100%
154 complete data set (although missing data are still present in the second dataset).

155

156 The molecular timeline for primate evolution that emerges from this study can be
157 interpreted with confidence. The dataset is sufficiently large to provide highly precise
158 branch length estimates, and the methods used are robust in accommodating violations
159 of the molecular clock. The comparison of the two calibration strategies reveals their
160 impact on the results by giving different age estimates within the tree, though the
161 variation in inferred ages is not extreme. Which ages are considered most accurate will
162 depend in large part on the degree of confidence in the fossils and their placement. As
163 an unanticipated result of the study, the difference in age estimates for the deepest
164 nodes of the phylogeny differ markedly when comparing the molecular rate models,
165 with Bayesian model selection supporting the autocorrelated model. As with previous
166 studies over the past several decades, the ancestral primate lineage is hypothesized to
167 have survived the great K-Pg mass extinction event.

168

169

METHODS

170 Bayesian estimates of divergence times of Primates were obtained using a supermatrix
171 of molecular data with 372 species and 3.44 million base pairs (Mbp), combined with 17
172 fossil calibrations. The matrix is the result of merging the 372-species and 61 thousand
173 base-pairs (Kpb) data set of Springer et al. (2012) with a 10-species subset of the
174 genome-scale alignment of dos Reis, et al. (2012). Bayesian analyses were done using
175 the program MCMCTree (Yang 2007). We assessed the robustness of time estimates by

176 varying the clock model (strict clock, independent rates and correlated rates), and by
177 obtaining estimates under two fossil calibration strategies. Note that time estimates
178 were obtained in two steps: In the first step estimates were obtained for the small
179 phylogeny of 10 species with a long alignment (3.38 Mbp). The marginal posterior of
180 times was then used to construct the time prior in the second step for the 372-species
181 phylogeny with a shorter alignment (61 Kbp). This approach is almost the same as
182 analysing the fully concatenated alignment in one step (3.38 Mbp + 0.061 Mbp), but is
183 computationally less demanding. All alignments, tree topology and fossil calibrations
184 are available in Supplementary Material.

185

186 *Sequence Alignment and Tree Topology*

187 *Springer et al. (2012) alignment.*—We retrieved the sequence alignment of Springer, et
188 al. (2012), which is an extended version of the alignment of Perelman, et al. (2011). The
189 alignment has 372 species (367 primates and 5 outgroup species) and 79 gene segments
190 (69 nuclear and 10 mitochondrial). The composite lagomorph sequence (an outgroup)
191 was removed. We added a scandentian species (*Tupaia belangeri*), because its complete
192 genome is available in the alignment of dos Reis, et al. (2012), and because it has the 10
193 gene segments from the mitochondrial genome available (accession NC_002521). Many
194 of the nuclear gene segments in the alignment of Springer, et al. (2012) were mixtures of
195 introns, exons and UTRs, with out-of-frame indels in some exons. We manually curated
196 the exons, and separated the coding and non-coding segments of the alignment. These
197 adjustments were necessary to facilitate an informed partition-based analysis of the
198 data. Our modified version of Springer’s alignment was thus divided into 6 partitions:
199 (1) 1st and 2nd codon positions for mitochondrial genes; (2) 3rd positions for
200 mitochondrial genes; (3) mitochondrial RNA genes; (4) 1st and 2nd codon positions for
201 nuclear genes; (5) 3rd positions for nuclear genes; and (6) non-coding segments of
202 nuclear genes (UTRs and introns). The concatenated alignment has 372 species and is
203 61,132 base pairs long (missing data 27%, Table 2). Our partitioning into codon
204 positions and coding vs. non-coding sequences follows established recommendations
205 (Shapiro et al., 2006; Yang and Rannala, 2006; Nascimento et al., 2017).

206

207 *dos Reis et al. (2012) alignment.*—We retrieved the genome-scale sequence alignment of
208 dos Reis, et al. (2012) of 36 mammal species, from which we extracted the sequences for

209 9 primates and 1 scandentian. The dos Reis et al. (2012) alignment was prepared using
210 the highly curated mammalian genomes available in Ensembl. Though three additional
211 primate genomes have become available in this database in the time since the original
212 alignment was prepared, it is unlikely that their inclusion would change our results.
213 The nine species represented in our study provide comprehensive phylogenetic
214 representation of all major nodes in the primate tree and represent each of the higher-
215 level clades (Figure 1, inset). The original alignment has 14,632 nuclear, protein-coding
216 genes, from which we removed 43 genes that were already present in the Springer
217 alignment and 1 gene that was extremely long. All columns in the alignment with
218 ambiguous nucleotides were removed, though care was taken not to disrupt the reading
219 frame of the aligned coding sequences. The alignment was divided into two partitions:
220 (1) 1st and 2nd codon positions; and (2) 3rd codon positions. The final alignment has 10
221 species and is 3,441,106 base pairs long (missing data 0%, Table 2).

222
223 *Tree topology.*—The topology of the 372-species phylogeny was estimated by maximum
224 likelihood (ML) using RAxML v 8.0.19 (Stamatakis 2014) under the GTR+G model (Yang
225 1994b, a), using seven partitions (Table 2) and 100 bootstrap replicates.

227 *Fossil Calibrations and Time Prior*

228 The two fossil calibration strategies used in this study are summarized in Table 3. They
229 represent two different interpretations of the fossil record to construct calibrations for
230 use in molecular clock dating analyses. Calibration strategy A is novel to this study, and
231 calibration strategy B is based on the Primate calibrations of dos Reis, et al. (2012).
232 Detailed justifications for the novel calibrations are provided in Appendix 1.

233
234 *Fossil calibration strategy A.*—We used the fossil-based prior densities constructed by
235 Wilkinson, et al. (2011) to calibrate the ages of crown Primates and crown
236 Anthropoidea. The prior densities were constructed by modelling the processes of
237 speciation, extinction, fossil preservation, and rates of fossil discovery in Primates. The
238 effects of the K-Pg extinction were accounted for in the model. We calibrated six more
239 node ages by using uniform distribution densities with soft bounds (Yang and Rannala
240 2006). We set the probability of violating a minimum bound to 1%. Because maximum
241 bounds are based on weak evidence, we set the probability that a maximum bound is

242 violated to 10% or 20%. The crown Haplorrhini node was left with no calibration as the
243 branch separating that clade from crown Primates is very short and we wanted to avoid
244 truncation with the fossil-modelling density on crown Primates. The prior on the age of
245 crown Haplorrhini is instead set using the birth-death process with parameters $\lambda = \mu = 1$
246 and $\rho = 0$. These parameter values specify a uniform kernel density (Yang and Rannala
247 1997, equation 7).

248

249 *Fossil calibration strategy B.*—We used the same nine calibrations that dos Reis, et al.
250 (2012) used to calibrate the Primates and Scandentia clades. An additional calibration
251 based on †*Tarsius* sp. was used for the Haplorrhini node. For nodes with a minimum
252 bound only, modelled using a truncated Cauchy density, the spread parameter was set to
253 $c = 2$ (Inoue, et al. 2010). For maximum bounds the probability that the bound was
254 violated was set to 5%. There are other differences between strategies A and B (Table
255 1). For example, in A, we considered †*Sahelanthropus*, dated to 7.25 million years ago
256 (Ma), to be the oldest member of the human-chimpanzee clade and used it to calibrate
257 the clade accordingly, while in B, dos Reis, et al. (2012) used †*Orrorin* (5.7 Ma) instead.
258 In A, †*Chororapithecus* is given an age of 10 Ma, while in B it is given the younger
259 (perhaps more conservative) age of 7.25 Ma (Benton, et al. 2009). We note that the ages
260 of fossils and their relationships to extant groups are often controversial and cannot
261 overemphasize the degree to which differences of opinion among palaeontologists are
262 an important source of uncertainty in the construction of fossil calibrations, and
263 accordingly, divergence time estimates throughout the phylogeny.

264

265 *Calibrating the 372-species phylogeny.* —Strategies A and B were used to obtain time
266 estimates for the 10-species phylogeny using the 3.38 Mbp alignment. Then skew-t
267 densities were fitted by ML to the marginal posterior ages of each of the 9 internal nodes
268 in the 10-species phylogeny, and used to calibrate the corresponding nodes in the 372-
269 species tree. Eight additional fossil calibrations (Table 3) were used to calibrate
270 additional nodes in the 372-species tree. For nodes without calibrations, the time prior
271 was constructed using the birth-death process with parameters $\lambda = \mu = 1$ and $\rho = 0$.
272 Bayesian time estimation then proceeded on the 372-species tree and 61 Kbp alignment
273 as usual.

274

275

Rate Prior

276 The time unit is 100 My. For the 10-species analysis, the rate prior was set as follows:
277 the nuclear substitution rate at third codon positions in apes is roughly within 10^{-9}
278 substitutions per site per year (s/s/y) (Burgess and Yang, 2008). At first and second
279 codon positions it is about a fifth of the third position rate, or 2×10^{-10} s/s/y. This gives
280 roughly an overall rate of about 5×10^{-10} s/s/y for the three positions combined. We
281 thus used a diffuse gamma density $G(2, 40)$ with mean 0.05 and 95% prior credibility
282 interval (CI) 0.00606–0.139 (corresponding to 6.06×10^{-12} to 1.39×10^{-10} s/s/y). The
283 analysis was conducted under both the auto-correlated rates (AR) and independent
284 rates (IR) models. Parameter σ^2 in the AR and IR models was assigned a gamma prior
285 $G(1, 10)$. Note that the average rate for loci, μ_i , and σ_i^2 are assigned a gamma-Dirichlet
286 prior (dos Reis, et al. 2014b).

287

288 For the 372-species phylogeny, the rate prior was assigned as follows: the mitochondrial
289 substitution rate at third positions is about 20 times the rate at third positions in
290 nuclear genes or 2×10^{-8} . Assuming 1st and 2nd codon positions evolve at about a fifth of
291 the third position rate we get roughly 4×10^{-9} . The prior mean is then approximately
292 2.5×10^{-9} s/s/y, which is the weighted average (by number of sites) of the substitution
293 rates for the nuclear and mitochondrial partitions. We thus used a gamma density $G(2,$
294 $8)$ with mean 0.25 and 95% CI 0.0302–0.696. For σ^2 we used $G(1, 10)$. The rate priors
295 are summarised in Table 4.

296

MCMC and Bayesian Selection of Clock Model

298 MCMC analyses were carried out with the program MCMCTree (Yang 2007), using the
299 approximate likelihood method (dos Reis and Yang 2011). Convergence of the MCMC to
300 the posterior distribution was assessed by running the analyses multiple times.

301 MCMCTree runs were carried out without sequence data to calculate the joint prior of
302 node ages. Results from all analyses were summarised as posterior means and 95% CIs.

303

304 We have implemented marginal likelihood calculation by thermodynamic integration
305 (path sampling) in the program MCMCTree. This allows us to calculate Bayes factors
306 (BF) and posterior model probabilities to select for a clock model in the analysis. Details

307 of our implementation are given in Appendix 2. Extensive discussions on marginal
308 likelihood estimation by thermodynamic integration and stepping-stones (a related
309 method) in the phylogenetic context are given in Lartillot and Philippe (2006), Lepage,
310 et al. (2007) and Xie, et al. (2011). A detailed simulation study is given in Ho et al.
311 (2015).

312

313 Thermodynamic integration is computationally intensive as we must sample from the
314 power posterior $f(\theta) f(D|\theta)^\beta$, in a sampling path from the prior ($\beta = 0$) to the posterior (β
315 $= 1$). Because the approximation to the likelihood is not good when samples are taken
316 far away from the maximum likelihood estimate (dos Reis and Yang 2011), as it happens
317 when β is small, the approximation cannot be used in the calculation of the power
318 posterior. Thus, we use exact likelihood calculation on a smaller dataset of nine primate
319 species (inset of Fig. 1), for the six partitions of the Springer alignment (Table 2) to
320 perform the Bayesian selection of clock model. We use 64 β -points to construct the
321 sampling path from the prior to the posterior and calculate the marginal likelihoods for
322 the strict clock, and the AR and IR models.

323

324 *Effect of genome-scale data*

325 In a conventional statistical inference problem, the variance of an estimate decreases in
326 proportion to $1/n$, with n to be the sample size. Thus, as the sample size approaches
327 infinity, the variance of an estimate approaches zero and the estimate converges to the
328 true value. In divergence time estimation, which is an unconventional estimation
329 problem, the non-identifiability of times and rates means that the uncertainty in the
330 posterior of times does not converge to zero as the amount of molecular data (the
331 sample size) approaches infinity, but rather converge to a limiting value imposed by the
332 uncertainties in the fossil calibrations (Yang and Rannala, 2006; Rannala and Yang,
333 2007). For infinitely long alignments, an infinite-sites plot (a plot of uncertainty in the
334 time posterior, measured as the width of the CI, i.e., the difference between the 2.5% and
335 97.5% limits vs. the mean posterior of time) would converge onto a straight line. This
336 line represents the amount of uncertainty in time estimates for every 1 million years
337 (My) of divergence that is due solely to uncertainties in the fossil calibrations. We
338 calculate the infinite-sites plots for time estimates on the 372-species phylogeny to
339 study the effect of genome-scale data on the uncertainty of species-level time estimates.

340

341

RESULTS

342

A Timeline of Primate Evolution

343

344

345

346

347

348

349

350

351

352

353

354

355

356

357

358

359

360

361

362

363

364

365

366

367

368

369

370

371

The main time estimates for Primates clades are summarised in Table 5, and Figure 1 illustrates time estimates under the AR model and calibration strategy A (Figs. 2 - 4 show detailed timetrees for the major clades). Under calibration strategy A and the AR model, we find that crown Primates originated 79.2–70.0 million years ago (Ma), before the K-Pg event at 66 Ma. However, the diversification of the main clades occurred much later. Crown Anthropoidea originated 48.3–41.8 Ma, with its two main crown groups, Catarrhini (Old World monkeys and apes) and Platyrrhini (New World monkeys) originating at 35.1–30.4 Ma and 27.5–23.6 Ma respectively. Crown tarsiers originated 33.5–15.5 Ma. Crown Strepsirrhini date back to 66.8–58.8 Ma, with its two main crown groups, Lemuriformes and Lorisiformes, dating back to 61.6–52.7 Ma and 40.9–34.1 Ma respectively.

Calibration strategy B under the AR model gives similar node age estimates for the younger nodes in the tree (i.e. the 95% CI of node age overlap, Fig. 5 and Table 5). However, for the older nodes in the phylogeny (and in particular for Euarchonta, Primatomorpha, Primates, Haplorrhini, Lemuriformes and Lemuriformes minus aye-aye), strategy A produced older estimates (Figure 5). Under strategy B a pre-K-Pg origin of crown Primates is also favoured, although the posterior distribution of the age of crown Primates straddles the K-Pg boundary (71.4–63.9 Ma). The posterior probability for a pre-K-Pg origin of crown Primates is 80.0% under strategy B and 100% under strategy A.

Note that the two calibration strategies are in many cases based on the same fossils (Table 3), and the intervals defined by the fossil bounds overlap extensively between the two strategies. However, the seemingly small differences between the two strategies lead to noticeable differences in the posterior time estimates (Table 5, Fig. 5). In general, minimum bound constraints are older in strategy A than in strategy B (Table 3), and thus this may be the cause of the older time estimates in A vs. B. Constructing calibrations from uncertain fossil information is a subjective task, and different

372 interpretations of the fossil record will lead to different posterior time estimates. The
373 situation cannot be improved by adding more molecular data to the analysis, because
374 the problem is statistically unconventional as we are trying to estimate two confounded
375 parameters (times and rates) while the data are only informative about their product
376 (the branch length). Furthermore, truncation effects among calibration densities affect
377 construction of the time prior (Inoue, et al. 2010, Warnock, et al. 2015), and thus
378 different calibration strategies may produce different time priors.

379

380 *Time prior and effect of truncation and outgroups.*– User-specified calibration densities
381 usually do not satisfy the constraint that descendant nodes must be younger than their
382 ancestors, thus the dating methodology must ‘truncate’ the calibration densities to
383 satisfy the constraint to construct the time prior (Rannala, 2016). The result is that
384 user-specified calibration densities and marginal priors of node ages may look
385 substantially different. Figure 6 illustrates the effect of truncation on prior densities for
386 strategies A and B. For example, in strategy B, the calibration densities on Euarchonta
387 (the root of the phylogeny) and on Primates interact (the primate node has a Cauchy
388 calibration density with a heavy tail), and consequently the prior density on the age of
389 Euarchonta is pushed back (Fig. 6). The result is that the marginal prior age of
390 Euarchonta ranges from 136–78 Ma (Fig. 6) instead of 130–61.5 Ma as in the calibration
391 density (Table 3), while the upper age for the Primate prior is too old (127 Ma). In
392 contrast, under strategy A, the calibration density on Primates has a much lighter tail,
393 and thus the truncation effect with the Euarchonta node is minimal. The result is that
394 the marginal time prior and the corresponding calibration densities for the Primates and
395 Euarchonta nodes are very similar (Fig. 6). Similarly, under strategy B, the priors for
396 two other nodes (Anthropoidea and Human-Gorilla) that use the heavy-tailed Cauchy
397 calibrations have upper 95% limits that also appear unreasonably old (86.3 Ma and 25.0
398 Ma respectively). In general, calibration strategy A, which avoids using the long-tailed
399 Cauchy calibrations, has calibration densities that are much closer to the resulting
400 marginal priors, and thus strategy A results in a time prior which is much closer to the
401 fossil information as interpreted by the palaeontologist.

402

403 *A Set of Calibrations for Mitogenomic Phylogenetic Analysis.*– Mitogenomic markers are
404 widely used to construct phylogenies of closely related primate species with examples

405 seen in phylogeographic studies of diversification of primates in the Amazon
406 (Nascimento, et al. 2014) and in the timing of human diversification (Rieux, et al. 2014).
407 The posterior distributions obtained here for the 10-species genomic data are useful
408 calibrations for mitogenomic studies. Note that these cannot be used if the molecular
409 alignment contains nuclear data as the calibrations already contain the information from
410 nuclear genomes. The list of skew-t calibrations is provided in Table 6, together with
411 approximations based on the gamma distribution, which can be used in software that
412 does not implement skew-t calibrations (such as BEAST or MrBayes).

413

414 *Effect of the Clock Model*

415 In the auto-correlated clock (AR) model, rates for branches are assumed to evolve
416 according to a geometric Brownian diffusion process, where the rate for a particular
417 branch depends on the rate of its parent branch. Large rate changes from an ancestral
418 branch to its daughter branches are penalized. In the independent rate (IR) model, rates
419 for branches are assumed to evolve independently among branches, and sharp rate
420 changes from parent to daughter branch are not penalized. Posterior means and 95%
421 CIs for locus (partition) rates obtained under both clock models are given in Table 7.
422 The clock model has a strong impact on posterior time estimates, particularly for the
423 most ancient nodes in the phylogeny. Under the IR model, the ages of Euarchonta,
424 Primatomorpha, Primates, Haplorrhini and Strepsirrhini are substantially older than
425 those estimated under the AR model (Table 5 and Figure 7).

426

427 Results of Bayesian model selection of clock model using thermodynamic integration are
428 shown in Table 8. The AR model has the highest marginal likelihood in 5 out of the 6
429 partitions analysed, with the posterior model probability > 90% in two partitions, and
430 79%, 66%, 53% and 29% in the other four. When the six partitions are analysed in a
431 multi-partition dataset, the posterior probability is virtually 100% in favour of the AR
432 model. We note that ideally, the marginal likelihood calculations should have been
433 carried out on the complete dataset, but unfortunately, this is so computationally
434 expensive that it cannot be done in a feasible amount of time. Although the estimates are
435 based on the data subset, it appears unlikely that the results would change for the whole
436 data, given the consistent support for the AR model.

437

438

Effect of genome-scale data

439 Figure 8 shows the infinite-sites plot for the primate data analysed here. For calibration
440 strategy A, the eight primate nodes shared between the 10-species and 372-species
441 trees (i.e. the nodes constrained by the large genome-scale alignment, table 2) fall in an
442 almost perfectly straight line ($R = 0.992$, Fig. 8A). This indicates that for these nodes,
443 uncertainty in the time estimates is dominated by uncertainties in the fossil calibrations
444 rather than by uncertainties in the molecular data. For strategy A, a regression line
445 through the origin fitted to the eight data points is $w = 0.128t$, meaning that for every 1
446 My of divergence, 0.128 My are added to the CI width (Fig. 8A). On the other hand, when
447 considering all 371 nodes in the tree, the relationship between CI width and mean times
448 is far from linear, and the level of uncertainty is much higher. In this case, 0.277 My are
449 added to the CI width for every 1 My of divergence. The trend is similar under
450 calibration strategy B (Fig. 8B), albeit in this case there is in general more uncertainty in
451 time estimates (i.e. the slope of the regression lines is larger). This appears due to
452 strategy B being more conservative than strategy A, that is, some of the calibration
453 densities used in B are substantially wider, encompassing larger time ranges (Fig. 6).

454

455

DISCUSSION

456

A Phylogenomic View of Primate Divergences

457 A primary aim of this work was to study the effect of genome-scale data on divergence
458 time estimates on a species-level phylogeny. Given the wide availability of whole
459 genome data for a core-set of species, it is important to know whether the use of these
460 data for a subsample of lineages will be enough to reduce time uncertainties in a
461 species-level phylogeny to the theoretical limit. The results of figure 8 clearly indicate
462 this is not the case. Although for the core ancestral nodes in the Primate phylogeny, the
463 genome-scale alignments do constrain uncertainty in time estimates close to their
464 theoretical limit (so it is highly unlikely that adding additional molecular data for these
465 species will improve time estimates appreciably), for species without genome-scale
466 data, there are still substantial uncertainties left for family-level and genus-level
467 divergences in the tree. For some nodes, the CI-width is almost as large as the node age
468 (for example, for Tarsiidae, the node age is 23.8 Ma with CI-width 18 My, which is 76% of

469 the node age, table 5). Thus much work is still needed in order to improve time
470 estimates for the hundreds of more recent divergences in the tree. Furthermore,
471 application of morphological-based models for dating (Ronquist et al. 2012) and the
472 fossilised birth-death process (Heath et al. 2014) also offer exciting prospects and
473 challenges in obtaining time estimates for the species-level divergences (O'Reilly et al.
474 2015, dos Reis et al. 2016). Improving these estimates will be important in studies of
475 primate diversification rates and to correlate primate diversification events with major
476 geological events in the history of the Planet (such as glaciations, continental drift, the
477 closure the Panama isthmus, etc.).

478

479 *Sequential Bayesian Analysis versus Secondary Calibrations*

480 In this work we used the posterior of times obtained under a small dataset as the prior
481 of times in a second analysis under a large dataset. This approach is justified as long as
482 the datasets are independent under the likelihood model and as long as the datasets do
483 not overlap (that is, they share no genes). The use of the posterior in an analysis as the
484 prior for the next is a well-known feature of Bayesian inference (Gelman et al. 2013).
485 Consider data that can be split into two subsets, $D = (D_1, D_2)$, which are independent
486 under the likelihood model. The posterior distribution for parameter θ is

$$487 \begin{aligned} f(\theta|D) &\propto f(\theta)f(D_1|\theta)f(D_2|\theta) \\ &\propto f(\theta|D_1)f(D_2|\theta) \end{aligned} ,$$

488 where $f(\theta|D_1) \propto f(\theta)f(D_1|\theta)$ is the posterior distribution of θ when only D_1 are
489 analysed. It is apparent that using $f(\theta|D_1)$ as the prior when analysing D_2 leads to the
490 posterior for the joint data D . In other words, performing the analysis in one step (joint
491 analysis of D_1 and D_2) or in two steps (posterior under D_1 as prior under D_2) results in
492 the same posterior distribution.

493

494 The approach we used here to analyse the primate data is justified because the
495 likelihood model assumes that the sequence partitions are non-overlapping and
496 independent. However our approach is approximate. In multi-parameter models, the
497 posterior is a multidimensional distribution that may have a complex correlation
498 structure. Here we ignored the correlation structure of the nine times estimated using
499 the genomic data, and approximated the corresponding high-dimensional time posterior

500 as the product of the marginal densities of the times, although a truncation is applied to
501 ensure that descendants are younger than ancestors. Note that joint analysis of all the
502 partitions would have been preferable, but it is computationally prohibitive.

503

504 This Bayesian sequential analysis is different from the use of secondary calibrations in
505 some dating studies (Graur and Martin, 2004), where the secondary calibrations were
506 used as point calibrations (with the uncertainties on node age estimates ignored), and
507 where in many cases the data analysed under the secondary calibration was the same as
508 the data analysed to obtain the calibration in the first place. We stress that the Bayesian
509 sequential approach is justified only if the data subsets do not overlap. The
510 genes/sequences analysed in the first step must be different from those analysed in the
511 second step.

512

513 *Clock Model*

514 An interesting result from our study is the finding that the AR model fits the primate
515 data better than the IR relaxed-clock model. In the context of previous studies, Lepage,
516 et al. (2007) found, using Bayes factors and no fossil calibrations, that two AR relaxed
517 clocks (CIR and log-normal) fitted real data (eukaryotes, mammals and vertebrates)
518 better than IR models. More recently, Lartillot, et al. (2016) introduced a mixed relaxed
519 clock that has auto-correlated- and independent-rates components. In their analysis,
520 the mixed clock appeared to provide a better description of rate evolution in the
521 mammal phylogeny, however, they did not assess clock model fit with Bayes Factors.
522 Linder et al. (2011) found, also by using Bayes factors, that IR models better fit an
523 angiosperm phylogeny better than AR models. Additionally, they found that, when
524 analysed without fossil calibrations, the AR model fit an ape phylogeny better than the
525 IR model. However, when analysed with fossil calibrations, the IR model fit the ape data
526 better.

527

528 In the AR model the variance of the log-rate for branches is proportional to the time of
529 divergence, so that the variance is expected to be close to zero for closely related
530 species. In other words, the AR model allows for “local clocks” for closely related
531 species, while allowing the rate to drift substantially across distantly related clades.
532 This model is, from a biological point of view, quite appealing intuitively, and it also fits

533 anecdotal evidence where the strict clock cannot be statistically rejected among very
534 closely related species, for example, among the apes (dos Reis, et al. 2016, box 2). In
535 contrast, the IR model assumes that the variance of the branch rates is the same for
536 different time scales. This would appear biologically unrealistic. Arguments have been
537 put forward in favour and against both of the two types of relaxed-clock models
538 examined by our study (Thorne et al. 1998, Drummond et al. 2006, Ho 2009), and
539 clearly further research is still needed to understand which clock model is the most
540 biologically realistic and appropriate for real data analysis. This will be a challenging
541 task given how difficult it has been to distinguish between the two models in simulation
542 studies (Heat et al. 2012, Ho et al. 2015, Lepage et al. 2007).

543

544 *Five Decades of Primate Molecular Timetrees*

545 The project of employing genomic information for discovering the geological age of the
546 Primates began virtually simultaneously with the publication of Zuckerkandl and
547 Pauling's (1965) molecular clock hypothesis. Sarich and Wilson (1967) employed a
548 strict clock interpretation of immunological distance data to hypothesize that humans
549 and other African apes (i.e., chimp and gorilla) shared a common ancestor as recently as
550 five million years ago. This was revolutionary at the time given the implications for the
551 necessarily rapid evolution of bipedal locomotion in the hominin lineage, and
552 accordingly, drew considerable attention from anthropological community (Read and
553 Lestrel, 1970; Uzzell and Pilbeam, 1971; Lovejoy et al., 1972; Radinsky, 1978; Corruccini
554 et al, 1980). Despite this interest, it wasn't until the 1980s that the field of divergence
555 time estimation assumed a relatively modern flavour. It was only then that investigators
556 began to apply statistical models to DNA sequence data for the purposes of branch
557 length and divergence time estimation (e.g., Hasegawa et al., 1985). Remarkably, these
558 studies first emerged at a time when the sister-lineage relationship of humans to chimps
559 was considered highly controversial (e.g., Goodman et al., 1983) — a relationship that is
560 now considered unequivocal.

561

562 From this point forward, primate timetrees have been produced with increasing
563 frequency, though with widely varying conclusions regarding the age of the last common
564 ancestor of Primates and of the major subclades within the Order (Table 1). Prior to the
565 study reported here, the estimated age of the living primate clade has spanned a 30 My

566 differential, ranging from as young as 55 Ma (Koop et al., 1989) to as old as 87 Ma
567 (Perelman et al, 2011). The new millennium has been a particularly active time for
568 primate divergence time analysis. Beginning in the early 2000's, published studies have
569 employed a diverse assortment of datasets applied to the problem (e.g., nuclear,
570 mitochondrial, and their combination), as well as a range of statistical methods and
571 calibration densities. Despite this array of data and methods, all of these studies—with
572 only one notable outlier (Chatterjee, 2009)—have consistently indicated that the crown
573 Primates clade originated prior to the K-Pg event (see also Steiper and Seiffert, 2012).
574 Given the continued dearth of fossil data to support this hypothesis, however, the result
575 continues to be viewed with scepticism by the paleoanthropological community (Bloch
576 et al., 2007; Silcox, 2008; O'Leary et al., 2013; but see Martin et al., 2007).

577

578 As described at length above, the current study gives added weight to the conclusion
579 that primates are an ancient clade of placental mammals, arising just prior to or millions
580 of years before the K-Pg. And even though lineage diversification within the major
581 subclades is hypothesized not to have occurred until after the commencement of the
582 Paleogene, the separation of tarsiers from other haplorrhines, and the divergence of
583 haplorrhines and strepsirrhines, consistently appear to proceed or nearly coincide with
584 the K-Pg. Given that this event was unequivocally one of the most disruptive and
585 destructive geological episodes in Earth history, the temporal coincidence speaks both
586 to the ecological flexibility and to the evolutionary opportunism of the earliest primates.
587 Although now extinct in North America and in Europe, the primate fossil record shows
588 that the clade was once nearly pan-global, even potentially including Antarctica. Thus,
589 when viewed in the context of divergence date estimates, all of which fall within a
590 temporal window when, as now, continental and island residences would have already
591 been sundered by significant oceanic barriers (most notably, the separation of South
592 America from Africa by the Atlantic Ocean), we must conclude that early primates would
593 have been able dispersers. In fact, the ability to cross barriers, both terrestrial and
594 aquatic, and to successfully colonize new land masses, are distinct hallmarks of the
595 primate radiation (Gingerich, 1981; Yoder and Nowak, 2006; de Queiroz, 2005, 2014;
596 Seiffert, 2012; Beard, 2016; Bloch et al., 2016).

597

598

599

SUPPLEMENTARY MATERIAL

600 Data available from the Dryad Digital Repository:

601 [http://dx.doi.org/10.5061/dryad.\[NNNN\]](http://dx.doi.org/10.5061/dryad.[NNNN])

602

603

FUNDING

604 This work was supported by grant BB/J009709/1 from the Biotechnology and
605 Biosciences Research Council (UK). Part of this work was carried out while Mdr was
606 visiting the National Evolutionary Synthesis Center (NESCent, National Science
607 Foundation #EF-0905606) in summer 2013. JBM was supported by a joint scholarship
608 from University College London and the Government of Mexico's CONACYT. ADY was
609 supported by a grant from the Burroughs Wellcome Fund and by DEB-1354610 from the
610 National Science Foundation.

611

612

DEDICATION

613 This paper is dedicated to the memory of our co-author Gregg F Gunnell.

614

615

APPENDIX 1

616 Justifications for dates assigned to 17 fossil calibrations in this study (Table 3) are given
617 below: 8 calibrations for strategy A (SA), 1 calibration for strategy B (SB), and 8
618 calibrations shared among both strategies (SAB). The justifications for the remaining
619 calibrations in Table 3 are given in dos Reis et al. (2012; see also Benton et al. 2009). In
620 some cases, the dates used are not exactly those published in cited references. In these
621 cases, the dates utilized reflect published as well as unpublished information or
622 adjustments deemed necessary given the uncertainty of some dates. In any case the
623 discrepancies are always small and unimportant considering the breadth of the fossil
624 calibrations. Note that specifying maximum bounds is a difficult task, in particular
625 because absence of fossil evidence is not evidence that a clade did not exist in a point in
626 time (Ho and Philips, 2009). We use stem fossils as benchmark points onto which to
627 construct diffuse maximum bounds (i.e. with a large probability of violation, p_{ij}) on some
628 node ages.

629

630 **Hominini | *Homo-Pan* | 7.5 Ma - 10 Ma | SA**

631 The minimum age for the divergence of hominins is placed at 7.5 Ma and is based on the
632 appearance of †*Sahelanthropus* at 7.2 Ma (Brunet, et al. 2002, Brunet, et al. 2005,
633 Lebatard, et al. 2008). There is some controversy as to the proper taxonomic position of
634 *Sahelanthropus* (Wolpoff, et al. 2006, MacLatchy, et al. 2010) but we regard it as the
635 oldest record of a plausible crown hominin. *Sahelanthropus* comes from the
636 Anthracotheriid Unit of an unnamed formation in the Mega-Chad Basin in Chad (Brunet,
637 et al. 2005). The associated mammalian fauna is very similar to that found from the
638 Nawata Formation, Lothagam, Kenya which may be as old as 7.4 Ma (MacDougall 2003).
639 The divergence of the hominin lineage seems unlikely to have occurred before the
640 appearance of the potential gorillin *Chororapithecus* at 10 Ma (Suwa, et al. 2007,
641 Harrison 2010a).

642

643 **Homininae | *Gorilla-Homo* | 10 Ma - 13.2 Ma | SA**

644 The minimum age for the divergence of crown hominines is placed at 10 Ma based on
645 the appearance of the potential gorillin *Chororapithecus*. Like *Sahelanthropus*, the
646 taxonomic status of *Chororapithecus* is not without controversy (Suwa, et al. 2007,
647 Harrison 2010a). Harrison (2010a) regards *Chororapithecus* as best interpreted as a
648 stem hominin or even a stem hominid – we feel that the features that do support a
649 relationship with gorillas are well enough established to use the date of appearance of
650 *Chororapithecus* as a minimum divergence date for hominines. *Chororapithecus* comes
651 from the late Miocene Beticha section of the Chorora Formation in Ethiopia and is dated
652 at 10-10.5 Ma (Geraads, et al. 2002). We use a maximum divergence date of 13.2 (Raza,
653 et al. 1983) for *Sivapithecus* but it is now evident that this date might be slightly too old.
654 In light of this the divergence of the hominine lineage is unlikely to have taken place
655 before the earliest appearance of the probable crown pongine *Sivapithecus* at 12.5 Ma
656 (Begun 2010, Begun, et al. 2012).

657

658 **Hominidae | *Pongo-Homo* | 11.2 Ma - 28 Ma | SA**

659 The minimum age for the divergence of crown hominids is placed at 11.2 Ma based on
660 the earliest appearance of the crown pongine *Sivapithecus* (Kappelman, et al. 1991,
661 Begun 2010, Begun, et al. 2012). *Sivapithecus* is known from Siwalik group rocks (Chinji,
662 Nagri and Dhok Pathan formations) in Indo-Pakistan that range in age from 14 Ma to 5.5

663 Ma (Badgley and Behrensmeyer 1995) with *Sivapithecus* restricted to a range of 12.5 Ma
664 to 7.4 Ma (Flynn, et al. 1995). The divergence of crown hominids is unlikely to have
665 occurred before the first appearance of *Kamoyapithecus* at 25 Ma (Seiffert 2010). We
666 use 28 Ma as a slightly more conservative maximum.

667

668 **Catarrhini | *Homo-Macaca* | 25 Ma - 33.7 Ma | SA**

669 The presence of the crown hominoid *Kamoyapithecus* (Zalmout, et al. 2010) indicates
670 that the minimum divergence time for crown Catarrhini is 25 Ma (Seiffert 2010).
671 *Kamoyapithecus* is only known from the Erageliet beds, Kalakol Basalts locality of
672 Lothidok in Kenya (Madden 1980, Leakey, et al. 1995, Rasmussen and Gutierrez 2009).
673 A soft maximum of 33.7 Ma on the age of crown catarrhines is given due to the absence
674 of hominoids before 33.7 Ma.

675

676 **Anthropoidea | Catarrhini-Platyrrhini | 41 Ma - 62.1 Ma | SA**

677 Calibration density constructed from fossil modeling. The effects of the K-Pg extinction
678 are included in the model. See Wilkinson, et al. (2011) for details.

679

680 **Haplorrhini | crown *Tarsius* | 45 Ma | SB**

681 The presence of the crown tarsiid *Xanthorhysis* in Shanxi Province, China (Beard 1998)
682 and apparently of the genus *Tarsius* in fissure fills at Shanghuang in Jiangsu Province,
683 China (Beard, et al. 1994), both dating to the late middle Eocene (40-45 Ma),
684 circumscribe the minimum divergence time for crown Haplorrhini at 45 Ma.

685

686 **Strepsirrhini | Lorisiformes-Lemuriformes | 37 Ma - 58 Ma | SA**

687 The minimum age for the divergence of crown Strepsirrhini is placed at 37 Ma based on
688 the first appearance of the crown lorisiform *Saharagalago* (Seiffert, et al. 2003).
689 *Saharagalago* is only known from Fayum Quarry BQ-2 in the Birket Qarun Formation,
690 Egypt. The divergence of crown strepsirrhines is unlikely to have occurred before the
691 first appearance of the basal primate *Altiatlasius* from Ouarzazate in Morocco which is
692 considered to represent the late Paleocene (Thanetian) and dating to around 58 Ma
693 (Gheerbrant, et al. 1993, Gheerbrant, et al. 1998, Seiffert 2010).

694

695 **Primates | Haplorrhini-Strepsirrhini | 57.6 Ma - 88.6 Ma | SA**

696 Calibration density constructed from fossil modeling. Includes the effects of the K-Pg
697 extinction in the model. See Wilkinson, et al. (2011) for details.

698

699 **Euarchonta | Scandentia-Primates | 65 Ma - 130 Ma | SA**

700 The minimum age for the divergence of crown Euarchonta is placed at 65 Ma based on
701 the first appearance of the crown euarchontan *Purgatorius* (Bloch, et al. 2007).

702 *Purgatorius* is known from the early Paleocene (Puercan) Tullock and Bear Formations
703 in Montana (Clemens 1974, Buckley 1997, Clemens 2004, Chester, et al. 2015) and from
704 the earliest Paleocene Ravenscrag Formation in Saskatchewan (Fox and Scott 2011). The
705 divergence of Euarchonta is unlikely to have been before the appearance of placental
706 mammals by at least 130 Ma (Luo 2007, but see Luo, et al. 2011 for a potential 130 My
707 old eutherian).

708

709 **Lorisidae | Nycticebus-Perodicticus | 14 Ma - 37 Ma | SAB**

710 The minimum age for the divergence of crown Lorisidae is placed at 14 Ma based on an
711 undescribed genus and species from Fort Ternan in Kenya cited by Walker (1978) and
712 Harrison (2010b). The minimum age could possibly be as old as 19 Ma if *Mioeuoticus*
713 (Leakey in Bishop 1962, Walker 1978) represents a crown lorid (Harrison 2010b).

714 Fossil lorids are known from the early to middle Miocene in Africa (Phillips and
715 Walker 2000, 2002, Harrison 2010b) and from the late Miocene of Pakistan (Jacobs
716 1981). The divergence of lorids is unlikely to have occurred before the first
717 appearance of the potential stem lorid *Karanisia* at BQ-2 in Egypt (Seiffert, et al. 2003).

718

719 **Galagidae | Galago-Euoticus | 15 Ma - 37 Ma | SAB**

720 The minimum age for the divergence of crown Galagidae is placed at 15 Ma based on an
721 undescribed genus and species from Maboko Island in Kenya cited by McCrossin (1999)
722 and Harrison (2010b). The minimum age could possibly be as old as 19 Ma if either

723 *Progalago* or *Komba* represent a crown galagid (MacInnes 1943, Simpson 1967,
724 Harrison 2010b). Fossil galagids are known from the early Miocene through early
725 Pleistocene in Africa (Phillips and Walker 2002, Harrison 2010b). The divergence of
726 galagids is unlikely to have occurred before the first appearance of the potential stem
727 lorid *Karanisia* at BQ-2 in Egypt (Seiffert, et al. 2003).

728

729 **Lorisiformes | *Galago-Perodicticus* | 18 Ma – 38 Ma | SAB**

730 The minimum age for the divergence of crown Lorisiformes is placed at 18 Ma based on
731 the appearance of the potential crown loroid *Mioeuoticus* in the early Miocene of East
732 Africa (Harrison 2010b). The divergence of lorisiforms is unlikely to have occurred
733 before the first appearances of *Karanisia* at BQ-2 in Egypt (Seiffert, et al. 2003). We use
734 38 Ma as a conservative soft maximum.

735

736 **Platyrrhini | Pitheciidae-Callitrichidae | 15.7 Ma – 33 Ma | SAB**

737 The minimum age for the divergence of crown Platyrrhini is based on the first
738 occurrence of the crown pitheciine *Proteropithecina* dated at 15.7 Ma (Kay, et al. 1998,
739 Fleagle and Tejedor 2002). The minimum age could be as much 18 Ma if either (or both)
740 *Soriacebus* or *Carlocebus* represent crown pitheciins (Fleagle, et al. 1987, Fleagle 1990,
741 Bown and Fleagle 1993, Fleagle, et al. 1995, Rosenberger 2011). All of these taxa are
742 known from the early and middle Miocene of Argentina (Fleagle and Tejedor 2002). The
743 divergence of platyrrhines is unlikely to have occurred before the appearance of the
744 crown catarrhine *Catopithecus* (33 Ma, Fayum, Egypt) although a recently published
745 report has claimed a 36 Ma date for a stem platyrrhine from Peru (Bond, et al. 2015). It
746 remains unclear how this older date was derived, however, and requires further
747 substantiation.

748

749 **Atelidae | *Ateles-Alouatta* | 12.8 Ma – 18 Ma | SAB**

750 The minimum age for the divergence of crown Atelidae (as recognized by Rosenberger,
751 2011; subfamily Atelinae of others) is based on the first appearance of the crown atelid
752 *Stirtonia* (Hershkovitz 1970, Rosenberger 2011) at 12.8 Ma. Fossil atelids are known
753 from the middle Miocene of Colombia and the Quaternary of Brazil and the Greater
754 Antilles (MacPhee and Horowitz 2002). The divergence of atelids is unlikely to have
755 occurred before the first appearance of the potential stem or crown atelid *Soriacebus* at
756 18 Ma (Bown and Fleagle 1993, Fleagle, et al. 1995).

757

758 **Cebidae | *Cebus-Saimiri* | 12.8 Ma – 18 Ma | SAB**

759 The minimum age for the divergence of crown Cebidae is based on the first appearance
760 of the crown cebid *Neosaimiri* (Stirton 1951, Hartwig and Meldrum 2002) dated at 12.8
761 from La Venta, Colombia. There are several older potential crown cebids including

762 *Dolichocebus* and *Tremacebus* from Argentina and *Chilecebus* from Chile, all dated to
763 around 20 Ma but it remains unclear how these taxa relate to the crown group. Recently,
764 an additional potential crown cebid has been described from Panama (Bloch et al. 2016)
765 dated at 20.9 Ma, which if substantiated would push the potential maximum bound to at
766 least 21 Ma. Here we have accepted the notion that the divergence of cebids is unlikely
767 to have occurred before the first appearance of the potential stem or crown atelid
768 *Soriacebus* at 18 Ma (Bown and Fleagle 1993, Fleagle, et al. 1995) but acknowledge that
769 this date could be as old as 21-22 Ma.

770

771 **Cercopithecidae | Papionini-Cercopithecini | 5 Ma – 23 Ma | SAB**

772 The minimum age for the divergence of crown Cercopithecidae is based on the first
773 appearance of *Parapapio* in the late Miocene (5 Ma) at Lothagam, Kenya. It is potentially
774 possible that some specimens of *Parapapio* from Lothagam could be as old as 7.4 Ma
775 (Jablonski and Frost 2010). The divergence of cercopithecids is unlikely to have
776 occurred before the first appearance of the stem cercopithecoid *Prohylobates*. The oldest
777 documented *Prohylobates* specimens are from Wadi Moghra in the Qatarra Depression,
778 Egypt dated to approximately 19.5 Ma. However, we view *Kamoyapithecus*, dated at 25
779 Ma as a crown hominoid, which implies that at least stem cercopithecoids were in
780 existence at that time. Given the controversial nature of our views on *Kamoyapithecus*,
781 we have used a date of 23 Ma as the likely maximum divergence time for crown
782 cercopithecids.

783

784 **Colobinae | Colobini-Presbytini | 9.8 Ma – 23 Ma | SAB**

785 The minimum age for the divergence of crown Colobinae is based on the first
786 appearance of *Microcolobus* in the middle Miocene (9.8 Ma) at Ngeringerowa, Kenya
787 (Benefit and Pickford 1986, Jablonski and Frost 2010). The divergence of colobines is
788 unlikely to have occurred before the first appearance of the stem cercopithecoid
789 *Prohylobates*. The oldest documented *Prohylobates* specimens are from Wadi Moghra in
790 the Qatarra Depression, Egypt dated to approximately 19.5 Ma. However, we view
791 *Kamoyapithecus*, dated at 25 Ma as a crown hominoid, which implies that at least stem
792 cercopithecoids were in existence at that time. Given the controversial nature of our
793 views on *Kamoyapithecus*, we have used a date of 23 Ma as the likely maximum
794 divergence time for crown colobines.

795

796

APPENDIX 2

797

Here we briefly describe our new implementation of Bayes factor calculation in

798

MCMCTree. Our approach is the thermodynamic integration-Gaussian quadrature

799

method implemented recently in the program BPP. The mathematical details are given

800

in Rannala and Yang (2017).

801

802

In this paper, we compare different rate models, m_i , which differ only in the density of

803

the branch rates while the prior on divergence times and the sequence likelihood are the

804

same between the models. The posterior distribution of times (\mathbf{t}) and rates (\mathbf{r}) given the

805

sequence data D , and given a clock model m_i is thus

806

807

$$f(\mathbf{t}, \mathbf{r} | D, m_i) = \frac{1}{z_i} f(\mathbf{t}) f(\mathbf{r} | \mathbf{t}, m_i) f(D | \mathbf{t}, \mathbf{r}),$$

808

where

809

$$z_i = \int f(\mathbf{t}) f(\mathbf{r} | \mathbf{t}, m_i) f(D | \mathbf{t}, \mathbf{r}) d\mathbf{t} d\mathbf{r}$$

810

is the marginal likelihood of the data for model m_i . Let m_r be the model with highest

811

marginal likelihood, and let $\text{BF}_{ir} = z_i/z_r$ be the Bayes factor of model i over model r . Then

812

the posterior probability of model i is

813

$$\Pr(m_i | D) = \frac{z_i \Pr(m_i)}{\sum_j z_j \Pr(m_j)} = \frac{z_i / z_r \Pr(m_i)}{\sum_j z_j / z_r \Pr(m_j)} = \frac{\text{BF}_{ir} \Pr(m_i)}{\sum_j \text{BF}_{jr} \Pr(m_j)},$$

814

where the sum is over all models being tested, and $\Pr(m_i)$ is the prior model probability.

815

816

We calculate z_i by sampling from the power posterior

817

$$f_\beta(\mathbf{t}, \mathbf{r} | D, m_i) \propto f(\mathbf{t}) f(\mathbf{r} | \mathbf{t}, m_i) f(D | \mathbf{t}, \mathbf{r})^\beta, \quad 0 \leq \beta \leq 1$$

818

for a given β value. We choose K β_j values to integrate between 0 and 1 according to the

819

Gauss-Legendre quadrature rule. The estimate of $\log z_i$ is then given by the quadrature

820

formula

821

$$\log z_i \approx \frac{1}{2} \sum_{j=1}^K w_j \bar{\ell}_{\beta_j},$$

822 where w_j are the Gauss-Legendre quadrature weights, and $\bar{\ell}_{\beta_j}$ is the average of log-
823 likelihood values, ℓ_{β_j} , sampled from the power posterior with β_j . The standard error of
824 the estimate is given by

825
$$\text{S.E.} = \frac{1}{2} \sqrt{\sum_{j=1}^K w_j^2 \text{Var}(\ell_{\beta_j}) / \text{ESS}},$$

826 where the variance is calculated over the MCMC sample of ℓ_{β_j} , and ESS is the effective-
827 sample size of ℓ_{β_j} .

828

REFERENCES

- 829
830
831 Alfaro ME, Santini F, Brock C, Alamillo H, Dornburg A, Rabosky DL, Carnevale G, Harmon
832 LJ. 2009. Nine exceptional radiations plus high turnover explain species diversity
833 in jawed vertebrates. *Proc Natl Acad Sci U S A*, 106:13410-13414.
834 Andersen MJ, Shult HT, Cibois A, Thibault JC, Filardi CE, Moyle RG. 2015. Rapid
835 diversification and secondary sympatry in Australo-Pacific kingfishers (Aves:
836 Alcedinidae: Todiramphus). *R Soc Open Sci*, 2:140375.
837 Aris-Brosou S, Yang Z. 2002. Effects of models of rate evolution on estimation of
838 divergence dates with special reference to the metazoan 18S ribosomal RNA
839 phylogeny. *Syst Biol*, 51:703-714.
840 Badgley C, Behrensmeyer AK. 1995. Two long geological records of continental
841 ecosystems. *Palaeogeography, Palaeoclimatology, Palaeoecology*, 115:1-11.
842 Beard K. 1998. A new genus of Tarsiidae (Mammalia: Primates) from the middle Eocene
843 of Shanxi Province, China, with notes on the historical biogeography of tarsiers.
844 *Bull. Carnegie Mus. Nat. Hist*, 34:260-277.
845 Beard KC. 2016. Out of Asia: Anthropoid origins and the colonization of Africa. *Annual*
846 *Review of Anthropology* 45: 13.1-13.15.
847 Beard KC, Qi T, Dawson MR, Wang B, Li C. 1994. A diverse new primate fauna from
848 middle Eocene fissure-fillings in southeastern China. *Nature*, 368:604-609.
849 Begun DR. 2010. Miocene Hominids and the Origins of the African Apes and Humans. In:
850 Brenneis D, Ellison PT editors. *Annual Review of Anthropology, Volume 39*. Palo
851 Alto, Annual Reviews, p. 67-84.
852 Begun DR, Nargolwalla MC, Kordos L. 2012. European Miocene hominids and the origin
853 of the African ape and human clade. *Evolutionary Anthropology: Issues, News,*
854 *and Reviews*, 21:10-23.
855 Benefit BR, Pickford M. 1986. Miocene fossil cercopithecoids from Kenya. *American*
856 *Journal of Physical Anthropology*, 69:441-464.
857 Benton MJ, Donoghue PC. 2007. Paleontological evidence to date the tree of life. *Mol Biol*
858 *Evol*, 24:26-53.
859 Benton MJ, Donoghue PCJ, Asher RJ. 2009. Calibrating and constraining molecular clocks.
860 In: Hedges BS, Kumar S editors. *The Timetree of Life*. Oxford, England, Oxford
861 University Press, p. 35-86.
862 Bininda-Emonds OR, Cardillo M, Jones KE, MacPhee RD, Beck RM, Grenyer R, Price SA,
863 Vos RA, Gittleman JL, Purvis A. 2007. The delayed rise of present-day mammals.
864 *Nature*, 446:507-512.
865 Bishop W. 1962. The mammalian fauna and geomorphological relations of the Napak
866 volcanics, Karamoja. *Records of the Geological Survey of Uganda 1957-58*:1-18.
867 Bloch JL, Silcox MT, Boyer DM, Sargis EJ. 2007. New Paleocene skeletons and the
868 relationship of plesiadapiforms to crown-clade primates. *Proceedings of the*
869 *National Academy of Sciences of the United States of America*, 104:1159-1164.
870 Bloch JL, Woodruff ED, Wood AR, Rincon AF, Harrington AR, et al. 2016. First North
871 American fossil monkey and early Miocene tropical biotic interchange. *Nature*,
872 533:243-246.
873 Bond M, Tejedor MF, Campbell KE, Jr., Chornogubsky L, Novo N, Goin F. 2015. Eocene
874 primates of South America and the African origins of New World monkeys.
875 *Nature*, 520:538-541.
876 Bown TM, Fleagle JG. 1993. Systematics, biostratigraphy, and dental evolution of the
877 Palaeothentidae, later Oligocene to early-middle Miocene (Deseadan-

- 878 Santacrucian) caenolestoid marsupials of South America. *Memoir (The*
879 *Paleontological Society)*:1-76.
- 880 Brunet M, Guy F, Pilbeam D, Lieberman DE, Likius A, Mackaye HT, Ponce de Leon MS,
881 Zollikofer CP, Vignaud P. 2005. New material of the earliest hominid from the
882 Upper Miocene of Chad. *Nature*, 434:752-755.
- 883 Brunet M, Guy F, Pilbeam D, Mackaye HT, Likius A, Ahounta D, Beauvilain A, Blondel C,
884 Bocherens H, Boisserie J-R, *et al.* 2002. A new hominid from the upper Miocene of
885 Chad, central Africa. *Nature*, 418:145-151.
- 886 Buckley GA. 1997. A new species of *Purgatorius* (Mammalia; Primatomorpha) from the
887 lower Paleocene Bear formation, Crazy Mountains basin, south-central Montana. *J*
888 *Paleontol*, 71:149-155.
- 889 Burgess R, Yang Z. 2008. Estimation of hominoid ancestral population sizes under
890 Bayesian coalescent models incorporating mutation rate variation and
891 sequencing errors. *Mol. Biol. Evol.*, 25: 1979–1994.
- 892 Chatterjee HJ, Ho SY, Barnes I, Groves C. 2009. Estimating the phylogeny and divergence
893 times of primates using a supermatrix approach. *BMC evolutionary biology*,
894 9:259.
- 895 Chester SG, Bloch JI, Boyer DM, Clemens WA. 2015. Oldest known euarchontan tarsals
896 and affinities of Paleocene *Purgatorius* to Primates. *Proceedings of the National*
897 *Academy of Sciences of the United States of America*, 112:1487-1492.
- 898 Clemens WA. 1974. *Purgatorius*, an early paromyid primate (Mammalia). *Science*,
899 184:903-905.
- 900 Clemens WA. 2004. *Purgatorius* (Plesiadapiformes, Primates?, Mammalia), a Paleocene
901 immigrant into northeastern Montana: stratigraphic occurrences and incisor
902 proportions. *Bulletin of Carnegie Museum of Natural History*:3-13.
- 903 Corruccini RS, Baba M, Goodman M, Ciochon RL, Cronin JE. 1980. Non-linear
904 macromolecular evolution and the molecular clock. *Evolution*, 34:1216-1219.
- 905 de Queiroz A. 2005. The resurrection of oceanic dispersal in historical biogeography.
906 *Trends Ecol. Evol.*, 20:68–73
- 907 de Queiroz A. 2014. *The Monkey's Voyage: How Improbable Journeys Shaped the History*
908 *of Life*. New York: Basic Books.
- 909 Dornburg A, Beaulieu JM, Oliver JC, Near TJ. 2011. Integrating fossil preservation biases
910 in the selection of calibrations for molecular divergence time estimation. *Syst Biol*,
911 60:519-527.
- 912 dos Reis M, Donoghue PC, Yang Z. 2014a. Neither phylogenomic nor palaeontological
913 data support a Palaeogene origin of placental mammals. *Biol. Lett.*, 10:20131003.
- 914 dos Reis M, Donoghue PC, Yang Z. 2016. Bayesian molecular clock dating of species
915 divergences in the genomics era. *Nat Rev Genet*, 17:71-80.
- 916 dos Reis M, Inoue J, Hasegawa M, Asher R, Donoghue PC, Yang Z. 2012. Phylogenomic
917 data sets provide both precision and accuracy in estimating the timescale of
918 placental mammal phylogeny. *Proc. R. Soc. Lond. B. Biol. Sci.*, 279:3491-3500.
- 919 dos Reis M, Thawornwattana Y, Angelis K, Telford MJ, Donoghue PC, Yang Z. 2015.
920 Uncertainty in the Timing of Origin of Animals and the Limits of Precision in
921 Molecular Timescales. *Current biology : CB*, 25:2939-2950.
- 922 dos Reis M, Yang Z. 2011. Approximate likelihood calculation for Bayesian estimation of
923 divergence times. *Mol. Biol. Evol.*, 28:2161–2172.
- 924 dos Reis M, Yang Z. 2013. The unbearable uncertainty of Bayesian divergence time
925 estimation. *J. Syst. Evol.*, 51:30-43.

- 926 dos Reis M, Zhu T, Yang Z. 2014b. The impact of the rate prior on Bayesian estimation of
927 divergence times with multiple Loci. *Syst. Biol.*, 63:555-565.
- 928 Drummond A, Ho S, Phillips M, Rambaut A. 2006. Relaxed phylogenetics and dating with
929 confidence. *PLoS Biol.*, 4:e88.
- 930 Duchene S, Lanfear R, Ho SYW. 2014. The impact of calibration and clock-model choice
931 on molecular estimates of divergence times. *Mol. Phy. Evol.*, 78:277-289.
- 932 Eizirik E, Murphy WJ, Springer MS, O'Brien SJ. 2004. Molecular phylogeny and dating of
933 early primate divergences. *Anthropoid Origins*, Springer, p. 45-64.
- 934 Finstermeier K, Zinner D, Brameier M, Meyer M, Kreuz E, Hofreiter M, Roos C. 2013. A
935 mitogenomic phylogeny of living primates. *PloS one*, 8:e69504.
- 936 Fleagle JG. 1990. New Fossil Platyrrhines from the Pinturas Formation, Southern
937 Argentina. *Journal of human evolution*, 19:61-85.
- 938 Fleagle JG, Bown T, Swisher C, Buckley G. 1995. Age of the Pinturas and Santa Cruz
939 formations. *Congreso Argentino de Paleontología y Bioestratigrafía*, p. 129-135.
- 940 Fleagle JG, Powers DW, Conroy GC, Watters JP. 1987. New Fossil Platyrrhines from
941 Santa-Cruz Province, Argentina. *Folia Primatol*, 48:65-77.
- 942 Fleagle JG, Tejedor MF. 2002. Early platyrrhines of southern South America. *Cambridge
943 Studies in Biological and Evolutionary Anthropology*:161-174.
- 944 Flynn LJ, Barry JC, Morgan ME, Pilbeam D, Jacobs LL, Lindsay EH. 1995. Neogene Siwalik
945 Mammalian Lineages - Species Longevities, Rates of Change, and Modes of
946 Speciation. *Palaeogeogr Palaeocl*, 115:249-264.
- 947 Fox RC, Scott CS. 2011. A New, Early Puercan (Earliest Paleocene) Species of *Purgatorius*
948 (*Plesiadapiformes*, Primates) from Saskatchewan, Canada. *J Paleontol*, 85:537-
949 548.
- 950 Gelman A, Carlin JB, Stern HS, Dunson DB, Vehtari A, Rubin DB. 2013. Bayesian data
951 analysis. 3rd edition. CRC Press.
- 952 Geraads D, Alemseged Z, Bellon H. 2002. The late Miocene mammalian fauna of Chorora,
953 Awash basin, Ethiopia: systematics, biochronology and 40K-40Ar ages of the
954 associated volcanics. *Tertiary Research*, p. 113-122.
- 955 Gheerbrant E, Cappetta H, Feist M, Jaeger J-J, Sudre J, Vianey-Liaud M, Sigé B. 1993. La
956 succession des faunes de vertébrés d'âge paléocène supérieur et éocène inférieur
957 dans le bassin d'Ouarzazate, Maroc. *Contexte géologique, portée
958 biostratigraphique et paléogéographique. Newsletters on Stratigraphy*:33-58.
- 959 Gheerbrant E, Sudre J, Sen S, Abrial C, Marandat B, Sigé B, Vianey-Liaud M. 1998.
960 Nouvelles données sur les mammifères du Thanétien et de l'Yprésien du Bassin
961 d'Ouarzazate (Maroc) et leur contexte stratigraphique. *Palaeovertebrata*, 27:155-
962 202.
- 963 Gingerich PD. 1981. Eocene Adapidae, paleobiogeography, and the origin of South
964 American Platyrrhini; pp. 123-138. In: Ciochon RL and Chiarelli AB (eds.)
965 *Evolutionary Biology of the New World Monkeys and Continental Drift*. Plenum
966 Publishing Corporation, New York.
- 967 Goodman M, Braunitzer G, Stangl A, Schrank B. 1983. Evidence on human origins from
968 haemoglobins of African apes. *Nature*, 303: 546-548.
- 969 Goodman M, Porter CA, Czelusniak J, Page SL, Schneider H, Shoshani J, Gunnell G, Groves
970 CP. 1998. Toward a phylogenetic classification of Primates based on DNA
971 evidence complemented by fossil evidence. *Mol Phyl Evol*, 9:585-598.
- 972 Graur D, Martin W. 2004. Reading the entrails of chickens: molecular timescales of
973 evolution and the illusion of precision. *Trends Genet*, 20:80-86.

- 974 Harrison T. 2010a. Dendropithecoidea, proconsuloidea, and hominoidea. *Cenozoic*
975 *mammals of africa* edited by werdelin L, sanders W:429-469.
- 976 Harrison T. 2010b. Later Tertiary Lorisiformes. *Cenozoic mammals of Africa*:333-349.
- 977 Hartwig WC, Meldrum DJ. 2002. Miocene platyrrhines of the northern Neotropics.
978 *Cambridge Studies In Biological And Evolutionary Anthropology*:175-188.
- 979 Hasegawa M, Kishino H, Yano T. 1985. Dating the human-ape splitting by a molecular
980 clock of mitochondrial DNA. *J. Mol. Evol.*, 22:160-174.
- 981 Heath TA, Holder MT, Huelsenbeck JP. 2012. A Dirichlet Process Prior for Estimating
982 Lineage-Specific Substitution Rates. *Mol. Biol. Evol.*, 29:939-955.
- 983 Heath TA, Huelsenbeck JP, Stadler T. 2014. The fossilized birth–death process for
984 coherent calibration of divergence-time estimates. *Proceedings of the National*
985 *Academy of Sciences*, 111:E2957–E2966.
- 986 Hershkovitz P. 1970. Notes on Tertiary platyrrhine monkeys and description of a new
987 genus from the late Miocene of Colombia. *Folia Primatol*, 12:1-37.
- 988 Ho SY. 2009. An examination of phylogenetic models of substitution rate variation
989 among lineages. *Biol. Lett.*, 5:421–424.
- 990 Ho SY, Duchene S. 2014. Molecular-clock methods for estimating evolutionary rates and
991 timescales. *Mol Ecol*, 23:5947-5965.
- 992 Ho SY, Duchene S, Duchene D. 2015. Simulating and detecting autocorrelation of
993 molecular evolutionary rates among lineages. *Mol Ecol Resour*, 15: 688-696.
- 994 Ho SY, Phillips MJ. 2009. Accounting for calibration uncertainty in phylogenetic
995 estimation of evolutionary divergence times. *Syst Biol*, 58:367-380.
- 996 Ho SY, Phillips MJ, Drummond AJ, Cooper A. 2005. Accuracy of rate estimation using
997 relaxed-clock models with a critical focus on the early metazoan radiation. *Mol*
998 *Biol Evol*, 22:1355-1363.
- 999 Inoue J, Donoghue PCH, Yang Z. 2010. The impact of the representation of fossil
1000 calibrations on Bayesian estimation of species divergence times. *Syst. Biol.*,
1001 59:74-89.
- 1002 Jablonski N, Frost S. 2010. *Cercopithecoidea. Cenozoic mammals of Africa*. Berkeley:
1003 University of California Press. p:393-428.
- 1004 Jacobs LL. 1981. Miocene lorisid primates from the Pakistan Siwaliks. *Nature*, 289:585-
1005 587.
- 1006 Kappelman J, Kelley J, Pilbeam D, Sheikh KA, Ward S, Anwar M, Barry JC, Brown B, Hake
1007 P, Johnson NM, *et al*. 1991. The Earliest Occurrence of Sivapithecus from the
1008 Middle Miocene Chinji Formation of Pakistan. *Journal of human evolution*, 21:61-
1009 73.
- 1010 Kay RF, Johnson D, Meldrum DJ. 1998. A new pitheciin primate from the middle Miocene
1011 of Argentina. *Am J Primatol*, 45:317-336.
- 1012 Kishino H, Thorne JL, Bruno WJ. 2001. Performance of a divergence time estimation
1013 method under a probabilistic model of rate evolution. *Molecular biology and*
1014 *evolution*, 18:352-361.
- 1015 Koop BF, Tagle DA, Goodman M, Slightom JL. 1989. A molecular view of primate
1016 phylogeny and important systematic and evolutionary questions. *Molecular*
1017 *biology and evolution*, 6:580-612.
- 1018 Kumar S, Hedges SB. 1998. A molecular timescale for vertebrate evolution. *Nature*,
1019 392:917-920.
- 1020 Lartillot N, Philippe H. 2006. Computing Bayes factors using thermodynamic integration.
1021 *Syst. Biol.*, 55:195-207.

- 1022 Lartillot N, Phillips MJ, Ronquist F. 2016. A mixed relaxed clock model. *Philosophical*
1023 *transactions of the Royal Society of London. Series B, Biological sciences*, 371.
- 1024 Leakey MG, Ungar PS, Walker A. 1995. A new genus of large primate from the late
1025 Oligocene of Lothidok, Turkana District, Kenya. *J. Hum. Evol.*, 28:519-531.
- 1026 Lebatard AE, Bourles DL, Durringer P, Jolivet M, Braucher R, Carcaillet J, Schuster M,
1027 Arnaud N, Monie P, Lihoreau F, *et al.* 2008. Cosmogenic nuclide dating of
1028 *Sahelanthropus tchadensis* and *Australopithecus bahrelghazali*: Mio-Pliocene
1029 hominids from Chad. *Proceedings of the National Academy of Sciences of the*
1030 *United States of America*, 105:3226-3231.
- 1031 Lepage T, Bryant D, Philippe H, Lartillot N. 2007. A general comparison of relaxed
1032 molecular clock models. *Mol. Biol. Evol.*, 24:2669-2680.
- 1033 Linder HP, Hardy CR, Rutschmann F. 2005. Taxon sampling effects in molecular clock
1034 dating: An example from the African Restionaceae. *Mol. Phy. Evol.*, 35:569-582.
- 1035 Linder M, Britton T, Sennblad B. 2011. Evaluation of Bayesian models of substitution
1036 rate evolution: parental guidance versus mutual independence. *Systematic*
1037 *Biology*, 60: 329-342.
- 1038 Liu Y, Medina R, Goffinet B. 2014. 350 my of mitochondrial genome stasis in mosses, an
1039 early land plant lineage. *Mol Biol Evol*, 31:2586-2591.
- 1040 Lovejoy CO, Burstein H, Heiple KH. 1972. Primate phylogeny and immunological
1041 distance. *Science*, 176:803-805.
- 1042 Luo ZX. 2007. Transformation and diversification in early mammal evolution. *Nature*,
1043 450:1011-1019.
- 1044 Luo ZX, Yuan CX, Meng QJ, Ji Q. 2011. A Jurassic eutherian mammal and divergence of
1045 marsupials and placentals. *Nature*, 476:442-445.
- 1046 MacDougall IF, C.S. 2003. Numerical age control for the Miocene-Pliocene succession at
1047 Lothagam. In: Leakey MGH, J.M. editor. *Lothagam the Dawn of Humanity in*
1048 *Eastern Africa*. New York, Columbia University Press, p. 43-64.
- 1049 MacInnes DG. 1943. Notes on the East African primates. *J. East Afr. Uganda Nat. Hist*
1050 *Soc.*, 39:521-530.
- 1051 MacLatchy L, DeSilva J, Sanders W, Wood B. 2010. *Hominini. Cenozoic Mammals of*
1052 *Africa*. University of California Press, Berkeley:471-540.
- 1053 MacPhee RD, Horovitz I. 2002. Extinct quaternary platyrrhines of the Greater Antilles
1054 and Brazil. *CAMBRIDGE STUDIES IN BIOLOGICAL AND EVOLUTIONARY*
1055 *ANTHROPOLOGY*:189-200.
- 1056 Madden CT. 1980. *NewProconsul (Xenopithecus)* from the Miocene of Kenya. *Primates*,
1057 21:241-252.
- 1058 Marshall CR. 1990. The fossil record and estimating divergence times between lineages:
1059 maximum divergence times and the importance of reliable phylogenies. *J. Mol.*
1060 *Evol.*, 30:400-408.
- 1061 Marshall CR. 2008. A simple method for bracketing absolute divergence times on
1062 molecular phylogenies using multiple fossil calibration points. *Am Nat*, 171:726-
1063 742.
- 1064 Martin RD. 1993. Primate origins: plugging the gaps. *Nature*, 363:223-234.
- 1065 Martin RD, Soligo C, Tavaré S. 2007. Primate origins: Implications of a Cretaceous
1066 ancestry. *Folia Primatologica*, 78:277-296.
- 1067 McCrossin ML. 1999. Phylogenetic relationships and paleoecological adaptations of a
1068 new bushbaby from the middle Miocene of Kenya. *American Journal of Physical*
1069 *Anthropology*:195-196.

- 1070 Nascimento FF, Lazar A, SeuÃ¡nez HN, Bovincino CR. 2014. Reanalysis of the
1071 biogeographical hypothesis of range expansion between robust and gracile
1072 capuchin monkeys. *Journal of Phylogeography*, 42:1349-1357.
- 1073 Nascimento FF, dos Reis M, Yang Z. 2017. A biologist's guide to Bayesian phylogenetic
1074 analysis. *Nat Ecol Evol*, 1:1446-1454.
- 1075 O'Leary MA, Bloch JL, Flynn JJ, Gaudin TJ, Giallombardo A, et al., 2013. The placental
1076 mammal ancestor and the post-K-Pg radiation of placentals. *Science*, 339:662-
1077 667.
- 1078 O'Reilly J, dos Reis M, Donoghue PCJ. 2015. Dating tips for divergence time estimation.
1079 *Trends Genet*, 31: 637-650.
- 1080 Paradis E. 2013. Molecular dating of phylogenies by likelihood methods: a comparison of
1081 models and a new information criterion. *Mol Phylogenet Evol*, 67:436-444.
- 1082 Perelman P, Johnson WE, Roos C, SeuÃ¡nez HN, Horvath JE, Moreira MAM, Kessing B,
1083 Pontius J, Roelke M, Rumpler Y, et al. 2011. A molecular phylogeny of living
1084 primates. *PLoS Genet*, 7:e1001342 EP.
- 1085 Phillips EM, Walker A. 2000. A new species of fossil loridid from the miocene of east
1086 Africa. *Primates*, 41:367-372.
- 1087 Phillips EM, Walker A. 2002. Fossil loridoids. In: Hartwig WC editor. *The Primate Fossil
1088 Record*. Cambridge, Cambridge University Press, p. 83-95.
- 1089 Poux C, Douzery EJ. 2004. Primate phylogeny, evolutionary rate variations, and
1090 divergence times: A contribution from the nuclear gene IRBP. *Am. J. Phys.
1091 Anthropol.*, 124:1-16.
- 1092 Pozzi L, Hodgson JA, Burrell AS, Sterner KN, Raaum RL, Disotell TR. 2014. Primate
1093 phylogenetic relationships and divergence dates inferred from complete
1094 mitochondrial genomes. *Molecular phylogenetics and evolution*, 75:165-183.
- 1095 Prum RO, Berv JS, Dornburg A, Field DJ, Townsend JP, Lemmon EM, Lemmon AR. 2015. A
1096 comprehensive phylogeny of birds (Aves) using targeted next-generation DNA
1097 sequencing. *Nature*, 526:569-573.
- 1098 Purvis A. 1995. A composite estimate of primate phylogeny. *Philosophical transactions
1099 of the Royal Society of London. Series B, Biological sciences*, 348:405-421.
- 1100 Radinsky L. 1978. Do albumin clocks run on time? *Science*, 200:1182-1183.
- 1101 Rannala B. 2016. Conceptual issues in Bayesian divergence time estimation. *Phil Trans
1102 Roy Soc B*, 371: 20150134.
- 1103 Rannala B, Yang Z. 2007. Inferring speciation times under an episodic molecular clock.
1104 *Syst. Biol.*, 56:453-466.
- 1105 Rannala B, Yang Z. 2017. Efficient Bayesian Species Tree Inference under the
1106 Multispecies Coalescent. *Syst Biol*, 66:823-842.
- 1107 Rasmussen DT, Gutierrez M. 2009. A Mammalian Fauna from the Late Oligocene of
1108 Northwestern Kenya. *Palaeontogr Abt A*, 288:1-52.
- 1109 Raza SM, Barry JC, Pilbeam D, Rose MD, Shah SMI, Ward S. 1983. New Hominoid
1110 Primates from the Middle Miocene Chinji Formation, Potwar Plateau, Pakistan.
1111 *Nature*, 306:52-54.
- 1112 Read DW, Lestrel PE. 1970. Hominid phylogeny and immunology: a critical appraisal.
1113 *Science*, 168:578-580.
- 1114 Rieux A, Eriksson A, Li M, Sobkowiak B, Weinert LA, Warmuth V, Ruiz-Linares A, Manica
1115 A, Balloux F. 2014. Improved calibration of the human mitochondrial clock using
1116 ancient genomes. *Molecular biology and evolution*, 31:2780-2792.

- 1117 Ronquist F, Klopstein S, Vilhelmsen L, Schulmeister, Murray DL, Rasnitsyn P. 2012. A
1118 Total-evidence approach to dating with fossils, applied to the early radiation of
1119 the Hymenoptera. *Systematic Biology*, 61:973-999.
- 1120 Rosenberger A. 2011. Evolutionary Morphology, Platyrrhine Evolution, and Systematics.
1121 *Anat Rec*, 294:1955-1974.
- 1122 Rutschmann F, Eriksson T, Abu Salim K, Conti E. 2007. Assessing calibration uncertainty
1123 in molecular dating: The assignment of fossils to alternative calibration points.
1124 *Syst. Biol.*, 56:591-608.
- 1125 Sanderson MJ. 1997. A nonparametric approach to estimating divergence times in the
1126 absence of rate constancy. *Mol. Biol. Evol.*, 14:1218-1231.
- 1127 Sarich VM, Wilson AC. 1967. Immunological time scale for Hominoid evolution. *Science*,
1128 158:1200-1203
- 1129 Seiffert ER. 2010. Chronology of Paleogene mammal localities. *Cenozoic mammals of*
1130 *Africa*. Berkeley: University of California Press. p:19-26.
- 1131 Seiffert ER. 2012. Early primate evolution in Afro-Arabia. *Evolutionary Anthropology*,
1132 21:239-253.
- 1133 Seiffert ER, Simons EL, Attia Y. 2003. Fossil evidence for an ancient divergence of lorises
1134 and galagos. *Nature*, 422:421-424.
- 1135 Shapiro B, Rambaut A, Drummond AJ. 2006. Choosing appropriate substitution models
1136 for the phylogenetic analysis of protein-coding sequences. *Mol Biol Evol*, 23:7-9.
- 1137 Simpson GG. 1967. The Tertiary lorisiform primates of Africa. *Bull. Mus. Comp. Zool.*,
1138 136:39-62.
- 1139 Silcox MT. 2008. The biogeographic origins of Primates and Euprimates: East, West,
1140 North, or South of Eden?, pp. 199-231. In Dagosto M and Sargis EJ (eds.)
1141 *Mammalian Evolutionary Morphology: a Tribute to Frederick S. Szalay*. Springer-
1142 Verlag, New York.
- 1143 Soltis PS, Soltis DE, Savolainen V, Crane PR, Barraclough TG. 2002. Rate heterogeneity
1144 among lineages of tracheophytes: Integration of molecular and fossil data and
1145 evidence for molecular living fossils. *Proc Nat Acad Sci U S A*, 99:4430-4435.
- 1146 Springer MS, Meredith RW, Gatesy J, Emerling CA, Park J, Rabosky DL, Stadler T, Steiner
1147 C, Ryder OA, Janecka JE, *et al.* 2012. Macroevolutionary dynamics and historical
1148 biogeography of primate diversification inferred from a species supermatrix. *PLoS*
1149 *one*, 7:e49521.
- 1150 Stamatakis A. 2014. RAxML version 8: a tool for phylogenetic analysis and post-analysis
1151 of large phylogenies. *Bioinformatics*, 30:1312-1313.
- 1152 Steiper ME, Young NM. 2006. Primate molecular divergence dates. *Mol. Phylogenet.*
1153 *Evol.*, 41:384-394.
- 1154 Steiper ME, Seiffert ER. 2012. Evidence for a convergent slowdown in primate molecular
1155 rates and its implications for the timing of early primate evolution. *Proc. Nat.*
1156 *Acad. Sci. U.S.A.* 109:6006-6011.
- 1157 Stirton RA. 1951. Ceboid monkeys from the Miocene of Colombia. *Bull. Univ. Calif. Pub.*
1158 *Geol. Sci.*, 28:315-356.
- 1159 Suwa G, Kono RT, Katoh S, Asfaw B, Beyene Y. 2007. A new species of great ape from the
1160 late Miocene epoch in Ethiopia. *Nature*, 448:921-924.
- 1161 Thorne JL, Kishino H. 2002. Divergence time and evolutionary rate estimation with
1162 multilocus data. *Syst Biol*, 51:689-702.
- 1163 Thorne JL, Kishino H, Painter IS. 1998. Estimating the rate of evolution of the rate of
1164 molecular evolution. *Mol. Biol. Evol.*, 15:1647-1657.

- 1165 Uzzell T, Pilbeam D. 1971. Phyletic divergence dates of hominoid primates: a
1166 comparison of fossil and molecular data. *Evolution*, 25:615-635.
- 1167 Walker AC. 1978. Prosimian primates. *Evolution of African Mammals*. Cambridge,
1168 Harvard University Press, p. 90-99.
- 1169 Warnock RC, Parham JF, Joyce WG, Lyson TR, Donoghue PC. 2015. Calibration
1170 uncertainty in molecular dating analyses: there is no substitute for the prior
1171 evaluation of time priors. *Proc. Biol. Sci.*, 282:20141013.
- 1172 Wilkinson RD, Steiper ME, Soligo C, Martin RD, Yang Z, Tavaré S. 2011. Dating primate
1173 divergences through an integrated analysis of palaeontological and molecular
1174 data. *Syst. Biol.*, 60:16-31.
- 1175 Wolpoff MH, Hawks J, Senut B, Pickford M, Ahern J. 2006. An ape or the ape: is the
1176 Toumaï cranium TM 266 a hominid. *PaleoAnthropology*, 2006:36-50.
- 1177 Xie W, Lewis PO, Fan Y, Kuo L, Chen M-H. 2011. Improving marginal likelihood
1178 estimation for Bayesian phylogenetic model selection. *Syst. Biol.*, 60:150-160.
- 1179 Yang Z. 1994a. Estimating the pattern of nucleotide substitution. *J. Mol. Evol.*, 39:105-
1180 111.
- 1181 Yang Z. 1994b. Maximum likelihood phylogenetic estimation from DNA sequences with
1182 variable rates over sites: approximate methods. *J. Mol. Evol.*, 39:306-314.
- 1183 Yang Z. 2007. PAML 4: Phylogenetic analysis by maximum likelihood. *Mol. Biol. Evol.*,
1184 24:1586-1591.
- 1185 Yang Z, Rannala B. 1997. Bayesian phylogenetic inference using DNA sequences: a
1186 Markov chain Monte Carlo Method. *Mol. Biol. Evol.*, 14:717-724.
- 1187 Yang Z, Rannala B. 2006. Bayesian estimation of species divergence times under a
1188 molecular clock using multiple fossil calibrations with soft bounds. *Mol. Biol.*
1189 *Evol.*, 23:212-226.
- 1190 Yang Z, Yoder AD. 2003. Comparison of likelihood and Bayesian methods for estimating
1191 divergence times using multiple gene loci and calibration points, with application
1192 to a radiation of cute-looking mouse lemur species. *Syst. Biol.*, 52:705-716.
- 1193 Yoder AD, Nowak MD. 2006. Has vicariance or dispersal been the predominant
1194 biogeographic force in Madagascar? Only time will tell. *Annual Review of Ecology,*
1195 *Evolution and Systematics*, 37:404-431.
- 1196 Yoder AD, Yang Z. 2004. Divergence dates for Malagasy lemurs estimated from multiple
1197 gene loci: geological and evolutionary context. *Mol Ecol*, 13:757-773.
- 1198 Zalmout IS, Sanders WJ, Maclatchy LM, Gunnell GF, Al-Mufarreh YA, Ali MA, Nasser AA,
1199 Al-Masari AM, Al-Sobhi SA, Nadhra AO, *et al.* 2010. New Oligocene primate from
1200 Saudi Arabia and the divergence of apes and Old World monkeys. *Nature*,
1201 466:360-364.
- 1202 Zhang C, Stadler T, Klopstein S, Heath TA, Ronquist F. 2016. Total-Evidence Dating
1203 under the Fossilized Birth-Death Process. *Syst Biol*, 65:228-249.
- 1204 Zhou X, Xu S, Xu J, Chen B, Zhou K, Yang G. 2012. Phylogenomic analysis resolves the
1205 interordinal relationships and rapid diversification of the laurasiatherian
1206 mammals. *Syst Biol*, 61:150-164.
- 1207 Zuckerkandl E, Pauling L. 1965. Molecules as documents of evolutionary history. *J Theor*
1208 *Biol*, 8:357-366.
- 1209

Table 1. Overview of estimates of divergence times in Primates (in millions of years ago) for selected studies.

Study	Data/Analysis	Primates	Haplorrhini	Anthropoidea	Platyrrhini	Catarrhini	Homininae	Strepsirrhini	Lorisiformes	Lemuriformes
Sarich and Wilson (1967)	Immunological distance/strict clock						5			
Hasegawa, et al. (1985)	896 bp mtDNA/strict clock						3.7			
Koop, et al. (1989)	B-globin DNA sequences/strict clock	55		40		25				
Purvis (1995)	Super Tree Analysis	57.2		39.9		14.7	8.1	41.8	22.1	39.6
Kumar and Hedges (1998)	658 nuclear genes (analyzed individually)/strict clock				47.6		6.7			
Goodman et al. (1998)	60-80 Kbp globin gene region/local clocks	63	58	40			18	50	23	45
Yang and Yoder (2003)	2404 bp mtDNA/local clocks				57.6			69.9	38.9	64.8
Poux and Douzery (2004)	1278 bp nDNA/local clocks			56.7, 58.4				45.4, 46.7	13.8, 14.2	39.6, 40.7
Eizirik, et al. (2004)	8,182 bp nDNA/relaxed clock	77.2		43.6				59.6		
Steiper and Young (2006)	59.8 Kbp of genomic data/relaxed clock w/ autocorrelated rates	77.5		42.9	20.8	30.5	8.6	57.1		
Bininda-Emonds, et al. (2007)	51,089 bp mtDNA & nDNA/ad hoc relaxed clock	87.7								
Chatterjee, et al. (2009)	6,138 bp mtDNA & 2,157 bp nDNA/relaxed clock	63.7		42.8	26.6	23.4	10.7	51.6	37.5	46.2
Perelman, et al. (2011)	34,927 bp DNA/relaxed clock w/independent rates	87.2	81.3	43.5	24.8	31.6	8.3	68.7	40.3	58.6
Springer, et al. (2012)	69 nDNA genes; 10 mtDNA genes/relaxed clock w/ autocorrelated rates	67.8	61.2	40.6	23.3	25.1	8.0	54.2	34.7	50.0
dos Reis, et al. (2012)	14,644 genes w/ 20.6 Mpb/relaxed clock w/ autocorrelated rates	68.2	65.0	37.4		26.4	10.4	55.1	35.6	49.3
Finstermeier, et al. (2013)	complete mtDNA genomes/relaxed clock w/independent rates	66.2	63.0	45.3	22.0	32.0	8.4	56.9	34.5	47.1
Pozzi, et al. (2014)	complete mtDNA genomes/relaxed clock w/ autocorrelated rates	74.1	70.0	46.7	20.9	32.1	10.6	66.3	40.3	59.6
This Study (Strategy A)	3.4 million bp/ relaxed clock w/ autocorrelated rates	74.4	70.6	45.0	25.3	32.6	10.5	62.7	37.9	57.2
This Study (Strategy B)	3.4 million bp/ relaxed clock w/ independent rates	84.8	78.6	45.9	25.3	28.8	7.6	64.0	38.2	55.3

Notes: All estimates are mean estimates; see original works for confidence/credible intervals; all taxonomic designations signify crown nodes (Primates = the divergence of Strepsirrhini and Haplorrhini; Haplorrhini = the divergence of *Tarsiidae* from Anthropoidea; Platyrrhini; Catarrhini; Homininae = the divergence of *Gorilla* from *Pan+Homo*; Strepsirrhini = the divergence of Lorisiformes and Lemuriformes; Lorisiformes = the divergence of Galagidae and Lorisidae; Lemuriformes = the divergence of *Daubentonia* (the aye-aye) from other Malagasy lemurs.

Table 2. Sequence alignment summary

Alignment	Partition^a	Sites	Species	Missing data^b
Springer et al.	1. mit 1st+2nd	4,816	330	61.4%
	2. mit 3rd	2,408	330	61.4%
	3. mit RNA	2,169	220	45.7%
	4. nuclear 1st+2nd	16,309	239	53.8%
	5. nuclear 3rd	8,156	239	53.8%
	6. nuclear non-coding	27,274	220	46.3%
	Partitions 1-6	61,132	372	51.1% (68.8%)
dos Reis et al.	7. nuclear 1st+2nd	2,253,316	10	0.0%
	8. nuclear 3rd	1,126,658	10	0.0%
	Partitions 7-8	3,379,974	10	0.0% (97.3%)
Total		3,441,106	372	0.78% (96.8%)

a. For topology estimation with RAxML, we used seven partitions: partitions 1 to 3, then 4 and 7 as one partition, 5 and 8 as one partition, and partition 6 divided into two: UTRs and Introns. b. Numbers in brackets are the % missing data for RAxML. Note that MCMCTree only uses the species present in a partition to calculate the likelihood for the partition. In RAxML missing species in a partition are represented as sequences of only gaps in the partition, and thus the amount of missing data is larger.

Table 3. Fossil calibrations used in this study.

Calibration Strategy ^a	Crown Group	Minimum (Ma)	Maximum (Ma)	MCMCTree Calibration ^b
Strategy A	Human-Chimp ^c	7.5 († <i>Sahelanthropus</i>)	10 (unlikely before stem gorilla † <i>Chororapithecus</i>)	B(0.075, 0.10, 0.01, 0.20)
	Human-Gorilla ^c	10 († <i>Chororapithecus</i>)	13.2 (unlikely before stem hominid † <i>Sivapithecus</i>)	B(0.10, 0.132, 0.01, 0.20)
	Hominidae ^c	11.2 († <i>Sivapithecus</i>)	28 (unlikely before stem hominoid † <i>Kamoyapithecus</i>)	B(0.112, 0.28, 0.01, 0.10)
	Catarrhini ^c	25 († <i>Kamoyapithecus</i>)	33.7 (absence of hominoids)	B(0.25, 0.337, 0.01, 0.10)
	Anthropoidea ^c	41 (K-Pg fossil modeling ^c)	62.1 (K-Pg fossil modeling ^d)	ST(0.4754, 0.0632, 0.98, 22.85)
	Strepsirrhini ^c	37 († <i>Saharagalago</i>)	58 (unlikely before † <i>Altiatlasius</i>)	B(0.37, 0.58, 0.01, 0.10)
	Primates ^c	57.6 (K-Pg fossil modeling ^c)	88.6 (K-Pg fossil modeling ^d)	S2N(0.900, 0.65, 0.0365, -3400, 0.6502, 0.1375, 11409)
	Euarchonta ^c	65 († <i>Purgatorius</i>)	130 (absence of placentals)	G(36, 36.9)
Strategy B	Chimp-Human	5.7 († <i>Orrorin</i>)	10 (absence of hominines)	B(0.057, 0.10, 0.01, 0.05)
	Gorilla-Human	7.25 († <i>Chororapithecus</i>)	-	L(0.0725, 0.1, 2)
	Hominidae	11.2 († <i>Sivapithecus</i>)	33.7 (absence of pongines)	B(0.112, 0.337, 0.05, 0.05)
	Catarrhini	23.5 († <i>Proconsul</i>)	34 (absence of hominoids)	B(0.235, 0.34, 0.01, 0.05)
	Anthropoidea	33.7 († <i>Catopithecus</i>)	-	L(0.337, 0.1, 2)
	Haplorrhini ^a	45 († <i>Tarsius</i>)	-	L(0.45, 0.1, 2)
	Strepsirrhini	33.7 († <i>Karanisia</i>)	55.6 (absence of strepsirrhines)	B(0.337, 0.556, 0.01, 0.05)
	Primates	55.6 († <i>Altiatlasius</i>)	-	L(0.556, 0.1, 2)
Euarchonta	61.5 (carpolestids and plesiadapids)	130 (absence of placentals)	B(0.615, 1.30, 0.01, 0.05)	
Shared by both strategies	Lorises ^c	14 (Lorisiidae gen et sp. Nov)	37 (unlikely before † <i>Karanisia</i>)	B(0.14, 0.37, 0.01, 0.10)
	Galagos ^c	15 (Galagidae gen et sp. Nov)	37 (unlikely before † <i>Karanisia</i>)	B(0.15, 0.37, 0.01, 0.10)
	Lorisiiformes ^c	18 († <i>Mioeouticus</i>)	38 (unlikely before † <i>Karanisia</i> /† <i>Saharagalago</i>)	B(0.18, 0.38, 0.01, 0.10)
	Platyrrhini ^c	15.7 (stem Pitheciinae)	33 (unlikely before † <i>Catopithecus</i>)	B(0.157, 0.33, 0.01, 0.10)
	Atelidae ^c	12.8 († <i>Stirtonia</i>)	18 (unlikely before † <i>Soriacebus</i>)	B(0.128, 0.18, 0.01, 0.10)
	Cebidae ^c	12.8 († <i>Neosaimiri</i>)	18 (unlikely before † <i>Soriacebus</i>)	B(0.128, 0.18, 0.01, 0.10)
	Cercopithecinae ^c	5 († <i>Parapapio</i>)	23 (unlikely before	B(0.05, 0.23, 0.01, 0.10)

Colobinae ^c	9.8 († <i>Microcolobus</i>)	† <i>Prohylobates/Kamoyapithecus</i> 23 (unlikely before † <i>Prohylobates/Kamoyapotheics</i>)	B(0.098, 0.23, 0.01, 0.10)
------------------------	------------------------------	---	----------------------------

a. Calibration strategies A and B are applied to the nodes in the phylogeny of 10 species. The shared calibrations are applied to the large tree of 372 species. Ages are in millions of years ago (Ma).

b. $B(t_L, t_U, p_L, p_U)$ means the node age is calibrated by a uniform distribution bounded between a minimum time t_L , and a maximum time t_U , with probabilities p_L and p_U that the age is outside the bounds. $L(t_L, p, c, p_L)$ means the node age is calibrated by a truncated Cauchy distribution with minimum age t_L and parameters p and c , with the probability that the age is younger than the minimum bound to be $p_L = 5\%$ (Inoue, et al. 2010). $ST(a, b, c, d)$ means the node age is calibrated by a skew-t density with parameters a, b, c and d (Wilkinson, et al. 2011). $S2N(a, b, c)$ means the node age is calibrated by a mixture of two skew-normal distributions (Wilkinson, et al. 2011). $G(a, b)$ means the node age is calibrated by a gamma distribution with shape a and rate b .

c. Detailed justifications for these fossil calibrations are given in the appendix. For all other calibrations, justifications are in Benton, et al. (2009) and dos Reis, et al. (2012).

d. Calibration densities are the posterior distribution from a model of fossil preservation and discovery with species diversification that takes into account the effects of the K-Pg extinction in the model (Wilkinson, et al. 2011).

Table 4. Rate priors used in this study. Time unit is 100 million years.

Alignment	Mean locus rate, μ_i	σ_i^2
10-species (nuclear)	G(2, 40); mean 5×10^{-10} subs/site/year	G(1, 10)
372-species (nuclear and mitochondrial)	G(2, 8) ; mean 2.5×10^{-9} subs/site/year	G(1, 10)

Table 5. Divergence times of major Primate groups.

Node	Crown group	Strategy A, AR		Strategy B, AR		Strategy A, IR		Strategy B, IR	
375	Primates	74.4	(70.0 - 79.2)	67.6	(63.9 - 71.4)	90.6	(83.7 - 98.1)	84.8	(78.1 - 92.3)
376	Haplorrhini	70.6	(66.5 - 75)	64.1	(60.7 - 67.6)	83.8	(77 - 91.1)	78.6	(72.1 - 85.8)
377	Anthropoidea	45.0	(41.8 - 48.3)	40.9	(38.1 - 43.9)	49.9	(45.1 - 54.9)	45.9	(41.2 - 51.3)
378	Catarrhini	32.6	(30.4 - 35.1)	29.3	(27.1 - 32.2)	32.2	(29 - 35.8)	28.8	(25.5 - 32.7)
379	Cercopithecoidea (OW monkeys)	21.9	(19.9 - 25.4)	19.9	(18.1 - 22.1)	20.8	(17.8 - 24.2)	18.6	(16.2 - 21.3)
380	Cercopithecinae	16.2	(14.5 - 19.6)	14.8	(13 - 16.3)	14.2	(12.3 - 16.7)	12.6	(10.8 - 14.7)
445	Colobinae	16.4	(14.4 - 19.7)	14.9	(13.4 - 16.8)	14.8	(12.6 - 17.2)	10.2	(8.7 - 11.9)

500	Hominoidea (apes)	24.0	(22.2 - 26.1)	21.0	(18.6 - 23.3)	21.4	(19 - 24.2)	18.6	(16.2 - 21.2)
501	Hylobatidae (gibbons)	14.0	(11.8 - 16.6)	12.5	(10 - 14.8)	10.5	(8.6 - 13.2)	9.7	(7.6 - 12)
504	<i>Hylobates</i>	4.1	(3.1 - 5.4)	3.7	(2.7 - 4.7)	4.1	(3.4 - 5)	3.7	(3 - 4.6)
512	<i>Nomascus</i>	3.2	(2.3 - 4.5)	2.9	(2 - 4.1)	3.7	(2.6 - 5)	3.3	(2.3 - 4.6)
518	Hominidae (human-orang)	20.3	(18.8 - 22)	17.4	(15.3 - 19.6)	17.3	(15.5 - 19.6)	14.7	(12.7 - 16.7)
519	Homininae (human-gorilla)	10.5	(10 - 11.3)	8.3	(7.7 - 9.1)	10.2	(9.9 - 10.8)	7.6	(7 - 8.4)
520	Human-Chimp	7.9	(7.3 - 8.4)	6.0	(5.5 - 6.6)	7.3	(6.7 - 7.9)	5.6	(4.3 - 5.9)
523	Ponginae (orangs)	3.7	(2.5 - 5.1)	3.1	(2.1 - 4.4)	2.6	(1.8 - 3.8)	2.3	(1.5 - 3.3)
524	Platyrrhini (NW monkeys)	25.3	(23.6 - 27.5)	23.8	(22.2 - 25.5)	27.9	(25.1 - 32.6)	25.3	(23 - 28)
528	Callitrichidae	15.5	(14.1 - 17.2)	14.5	(13.3 - 15.9)	17.5	(15.6 - 19.6)	15.9	(14.1 - 17.9)
565	Cebidae	19.1	(17.7 - 21)	18.2	(17 - 19.6)	18.8	(17 - 21.1)	17.8	(16 - 19.6)
558	Aotidae (owl monkeys)	18.5	(17.1 - 20.3)	17.7	(16.3 - 19)	16.8	(14.1 - 18.8)	15.8	(13.5 - 18.1)
576	Atelidae	18.5	(17.1 - 20.3)	17.7	(16.3 - 19)	16.8	(14.1 - 18.8)	15.8	(13.5 - 18.1)
598	Pitheciidae	22.5	(20.8 - 24.7)	21.2	(19.7 - 22.9)	24.3	(20.6 - 32.5)	22.9	(19.6 - 22.9)
618	Tarsiidae (Tarsius)	23.8	(15.5 - 33.5)	21.4	(13.8 - 29.8)	22.2	(16.5 - 29.6)	20.1	(14.9 - 26.7)
624	Strepsirrhini	62.7	(58.8 - 66.8)	56.7	(53.8 - 59.9)	70.0	(63 - 78.4)	64.0	(56.9 - 72.2)
625	Lemuriformes	57.2	(52.7 - 61.6)	51.5	(48 - 55.1)	60.3	(52.8 - 68.4)	55.3	(48.4 - 63.3)
626	Lemuriformes minus Aye-aye	40.3	(34.8 - 45.8)	35.7	(30.3 - 41)	40.0	(35.5 - 45.2)	36.5	(32.1 - 41.6)
629	Cheirogaleidae	32.7	(27.3 - 38.2)	28.7	(23.5 - 34.4)	31.1	(26.5 - 35.9)	28.4	(24.1 - 33.1)
630	Cheirogaleidea (minus <i>Phaner</i>)	27.4	(22.7 - 32.2)	23.9	(19.7 - 28.9)	25.3	(21.9 - 29)	23.2	(19.9 - 26.9)
633	<i>Microcebus</i> (mouse lemurs)	10.4	(7.8 - 13.2)	8.9	(7 - 11.4)	9.6	(8.3 - 11.3)	8.7	(7.3 - 10.3)
657	<i>Cheirogaleus</i>	17.8	(13.1 - 23.2)	15.5	(11.4 - 20.8)	12.3	(8.8 - 17)	11.1	(8 - 15.1)
660	<i>Lepilemur</i>	15.3	(11.8 - 20.5)	13.3	(10.5 - 17.4)	13.0	(10.7 - 15.8)	11.5	(9.7 - 13.9)
683	Indriidae	27.1	(22.2 - 32.7)	23.9	(19.5 - 29.2)	21.2	(16.8 - 26.2)	19.3	(15.2 - 24)
697	Lemuridae	27.8	(23.1 - 33.3)	24.3	(19.4 - 29.4)	23.6	(20.1 - 27.9)	21.5	(18.1 - 25.2)
717	Lorisiformes	37.9	(34.1 - 40.9)	35.0	(30.2 - 38.2)	38.3	(34.5 - 41.9)	38.2	(30.8 - 38.5)
718	Galagidae	28.8	(24.7 - 31.9)	26.6	(21.7 - 30)	23.9	(20.6 - 27.5)	30.0	(22.3 - 30.4)
732	Lorisidae	35.9	(32.1 - 38.8)	33.2	(28.5 - 36.4)	35.2	(31.5 - 38.7)	36.4	(29.1 - 36.7)

Note: AR: Auto-correlated rates model. IR: Independent rates model. Times are posterior means in Ma. Numbers in brackets are 95% CI.

Table 6. Suggested skew-t and gamma calibrations for mitogenomic studies.

Crown group	Skew-t^{a,b}	Gamma^{a,c}
Primates	ST(0.878, 0.169, 2.41, 94.6)	G(78.6, 77.6)
Strepsirrhini	ST(0.580, 0.0567, 2.12, 149)	G(262, 327)
Haplorrhini	ST(0.705, 0.0628, 1.66, 960)	G(254, 411)
Anthropoidea	ST(0.415, 0.0291, 0.949, 294)	G(271, 363)
Catarrhini	ST(0.292, 0.0206, 0.995, 167)	G(316, 733)
Hominoidea	ST(0.185, 0.0167, 2.44, 312)	G(316, 1040)
Human-Gorilla	ST(0.0996, 0.0103, 19.6, 100)	G(311, 1575)
Human-Chimp	ST(0.0788, 0.00687, 3.51, 6.15)	G(292, 2715)

a. Densities calculated under fossil calibration strategy A and AR model using a time unit of 100 My.

b. The parameters of the Skew-t distribution are location, scale, shape and df.

c. Note that here we use the shape (α) and rate (β) parameterization. For the scale parameterization use $s = 1/\beta$. The mean is α/β and variance is α/β^2 .

Table 7. Posterior means of locus rates and rate variance parameters under calibration strategy A.

Partition	AR locus mean^a	AR locus σ^2	IR locus mean^a	IR locus σ^2
1. mit 1st+2nd	0.20 (0.086–0.38)	1.6 (1.1–2.2)	0.37 (0.33–0.41)	0.33 (0.26–0.41)
2. mit 3rd	1.8 (0.63–3.7)	4.6 (3.6–5.8)	3.0 (2.7–3.3)	0.24 (0.19–0.30)
3. mit RNA	0.53 (0.23–1.0)	1.8 (1.1–2.7)	0.54 (0.48–0.60)	0.31 (0.23–0.41)
4. nuclear 1st+2nd	0.11 (0.041–0.24)	2.4 (1.6–3.3)	0.037 (0.033–0.041)	0.37 (0.27–0.51)
5. nuclear 3rd	0.34 (0.13–0.71)	2.3 (1.6–3.1)	0.11 (0.098–0.12)	0.33 (0.23–0.47)
6. nuclear non-coding	0.20 (0.065–0.47)	3.3 (2.4–4.4)	0.068 (0.061–0.075)	0.40 (0.30–0.56)
7. nuclear 1st+2nd	0.038 (0.024–0.057)	0.26 (0.12–0.51)	0.027 (0.022–0.034)	0.14 (0.062–0.28)
8. nuclear 3rd	0.16 (0.099–0.23)	0.27 (0.12–0.54)	0.11 (0.090–0.14)	0.17 (0.077–0.33)

a. Substitutions per site per 100 My. For example 0.21 means 2.1×10^{-9} subs/site/year.

Table 8. Bayesian model selection of rate model.

Dataset	Model	Log Marginal L^a	BF	P^b
Mitochondrial 1 st and 2 nd c.p.	SC	-16,519.03 (0.010)	1.3×10^{-18}	1.2×10^{-18}
	IR	-16,480.58 (0.021)	0.063	0.060
	AR	-16,477.82 (0.035)	-	0.94
Mitochondrial 3 rd c.p.	SC	-16,684.50 (0.014)	-	0.61
	IR	-16,686.29 (0.043)	0.17	0.10
	AR	-16,685.26 (0.040)	0.47	0.29
Mitochondrial RNA	SC	-7,906.85 (0.0087)	0.74	0.39
	IR	-7,908.40 (0.015)	0.16	0.08
	AR	-7906.55 (0.023)	-	0.53
Nuclear 1 st and 2 nd c.p.	SC	-32,179.80 (0.0092)	0.0047	0.0037
	IR	-32,175.77 (0.022)	0.27	0.21
	AR	-32,174.44 (0.032)	-	0.79
Nuclear 3 rd c.p.	SC	-24,535.33 (0.012)	7.2×10^{-12}	6.7×10^{-12}
	IR	-24,512.45 (0.038)	0.062	0.058
	AR	-24,509.67 (0.030)	-	0.94
Nuclear UTR and introns	SC	-64,739.20 (0.016)	5.7×10^{-4}	3.8×10^{-4}
	IR	-64,732.41 (0.038)	0.51	0.34
	AR	-64,731.73 (0.046)	-	0.66
All ^c	SC	-162,684.8 (0.024)	2.1×10^{-103}	2.1×10^{-103}
	IR	-162,467.0 (0.086)	8.4×10^{-9}	8.4×10^{-9}
	AR	-162,448.4 (0.15)	-	1.00

Marginal likelihoods are estimated by thermodynamic integration with 64 points. The substitution model is HKY+G. SC: Strict clock; IR: Independent log-normal; AR: Auto-correlated rates. The age of the root is fixed to one (i.e. we use a 'B(0.99, 1.01)' calibration on the root in MCMCTree). The rate priors are G(2, 1) and G(2, 20) for mitochondrial and nuclear data respectively. The prior on σ^2 is G(1, 1) in all cases. The model with the highest posterior probability in each dataset is shown in bold type. a: Values in brackets are the standard errors (see Appendix 2). b: Posterior model probabilities are calculated assuming a uniform prior on models. c: The six datasets are analysed together as six partitions.

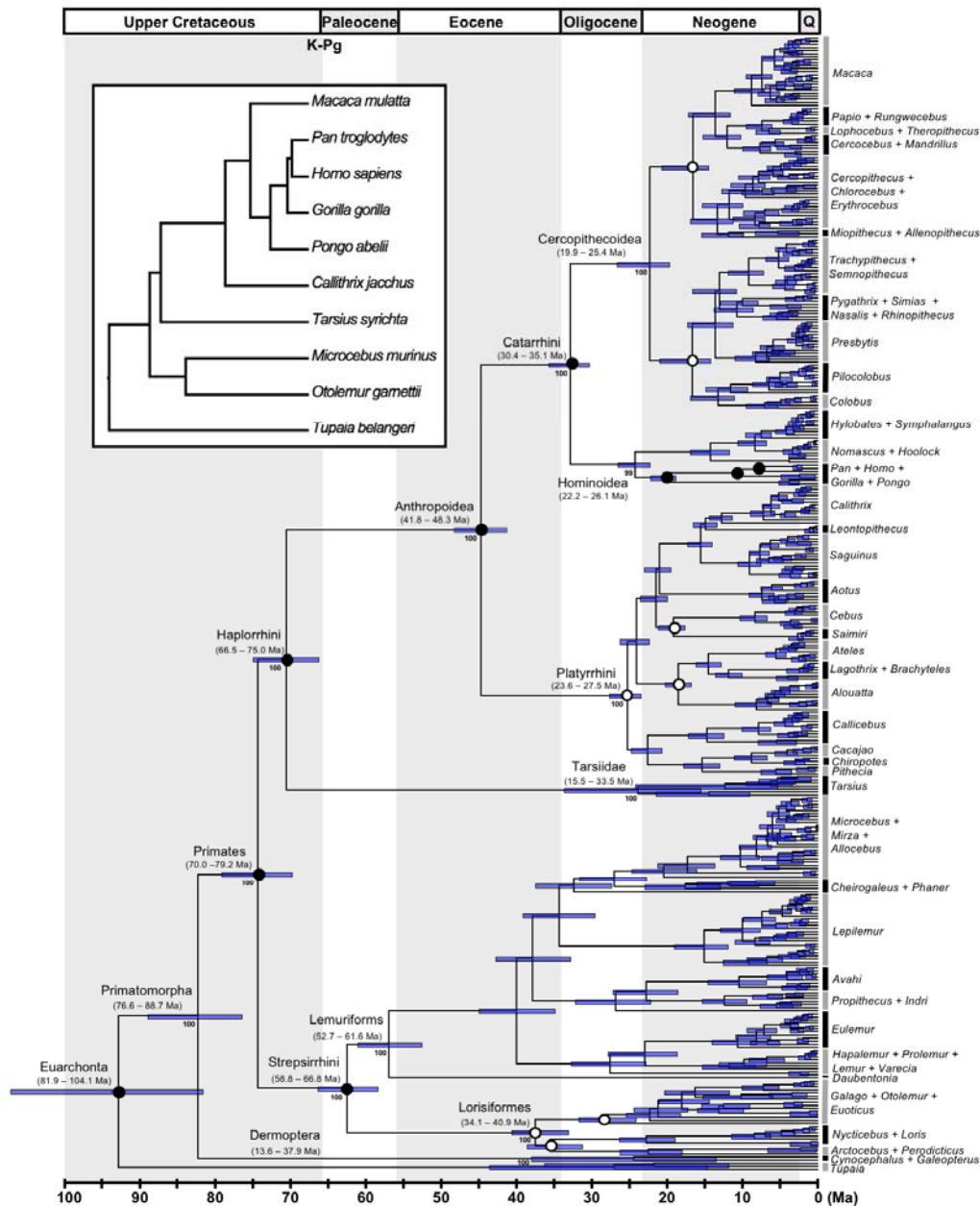


Figure 1.

Figure 1. The timetree of Primates. Nodes are drawn at their posterior mean ages in millions of years ago (Ma) estimated under the autocorrelated-rates (AR) clock model and calibration strategy A. Filled dots indicate nodes calibrated with the posterior times from the 10-species tree (inset figure), and empty dots indicate nodes with fossil constraints in the 372-species tree. Horizontal bars and numbers in parenthesis represent the 95% posterior CI for the node ages. Numbers associated with branches are ML Bootstrap support values of major clades.

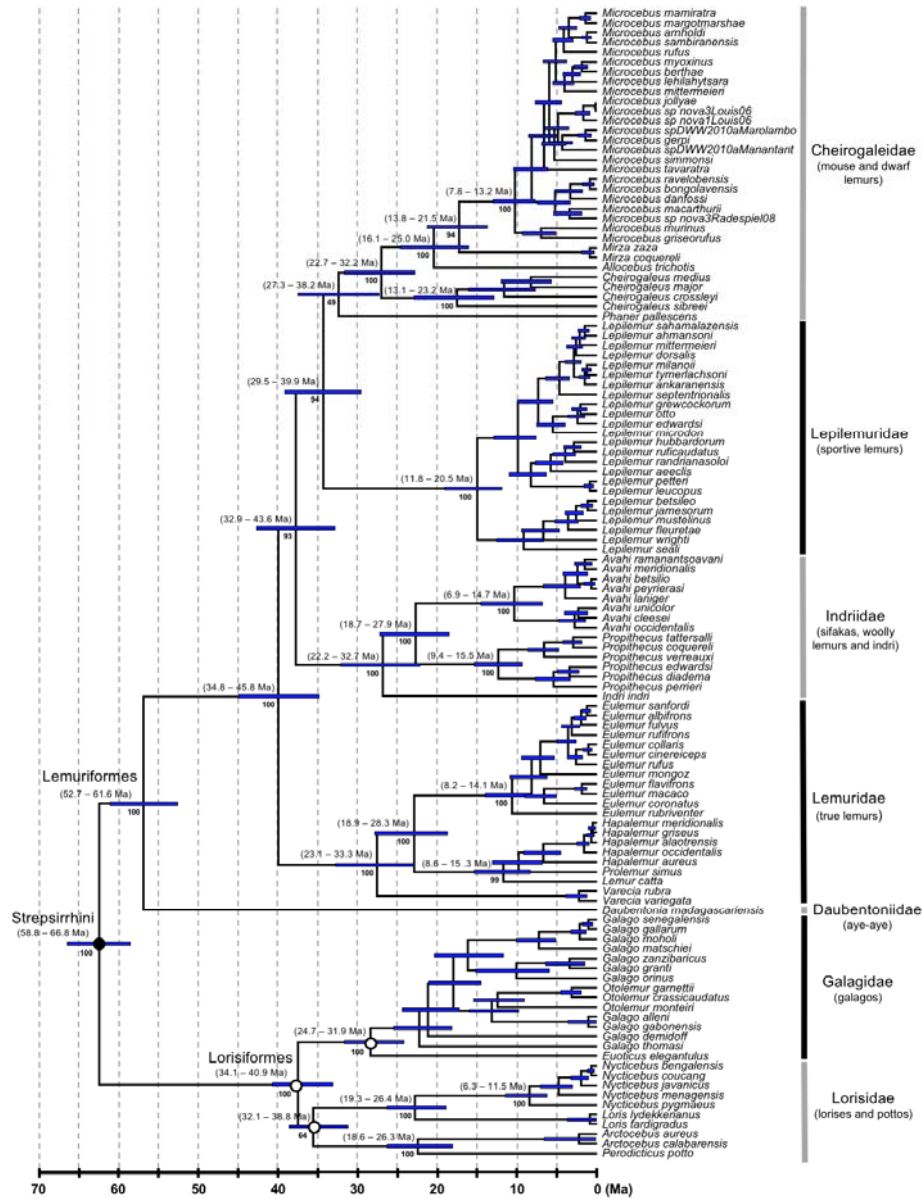


Figure 2.

Figure 2. Strepsirrhine portion of the primate timetree (AR clock and calibration strategy A). Legend as for figure 1.

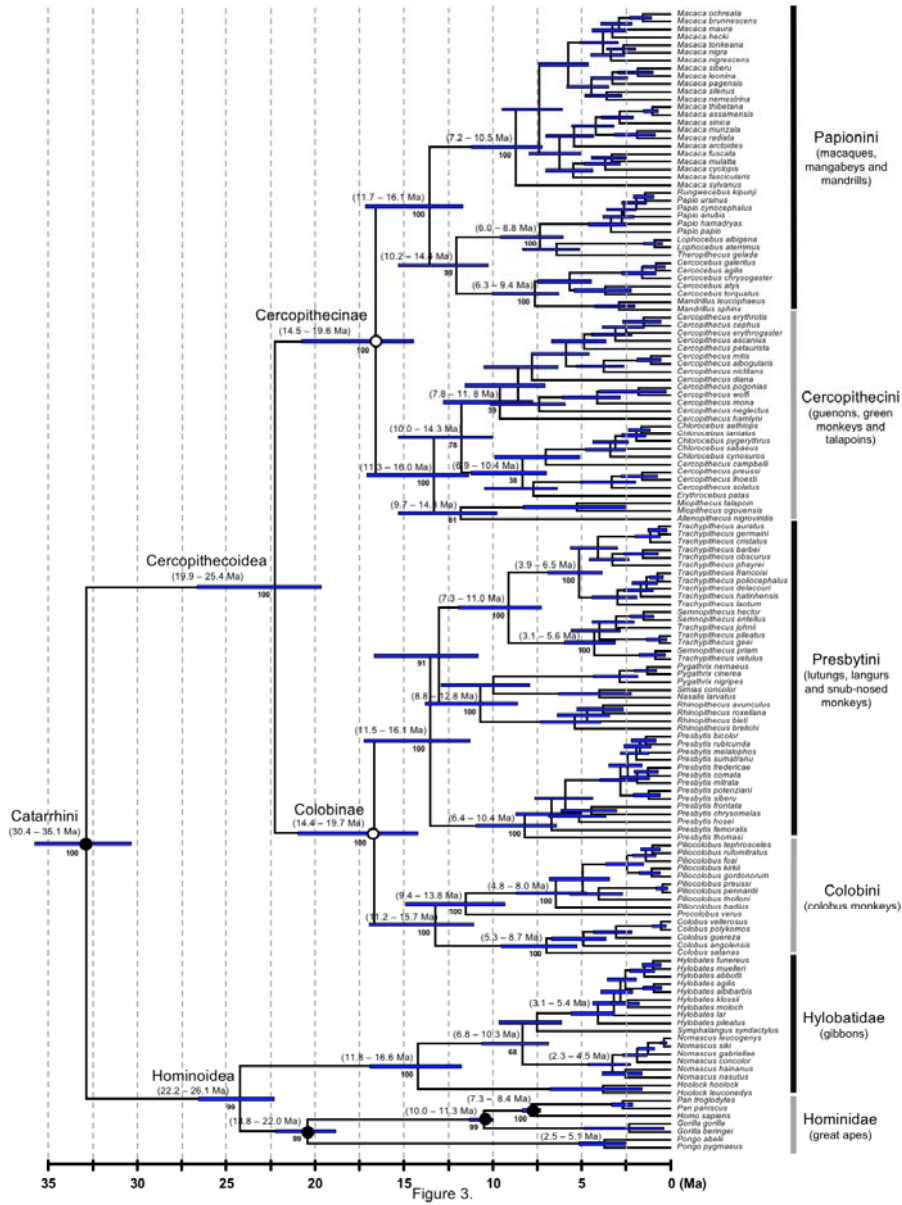


Figure 3. Catarrhine portion of the primate timetree (AR clock and calibration strategy A). Legend as for figure 1.

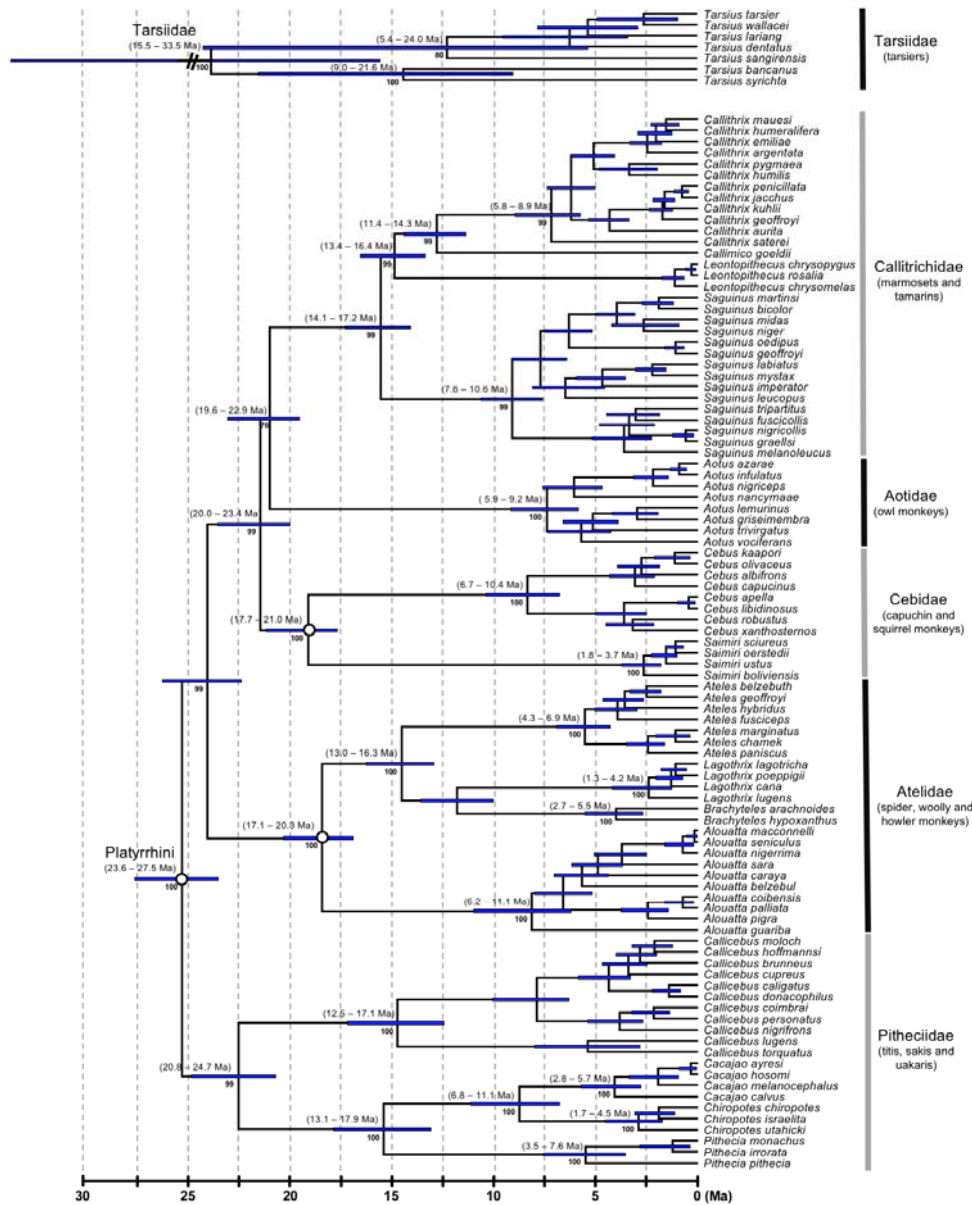


Figure 4.

Figure 4. Tarsiidae and platyrrhine portion of the primate timetree (AR clock and calibration strategy A). Legend as for figure 1.

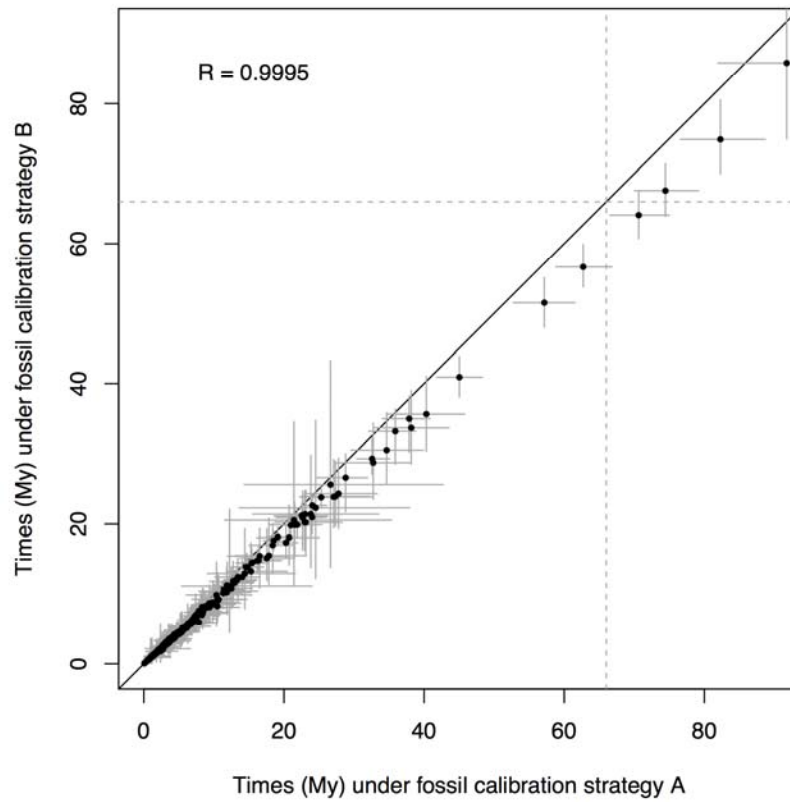


Figure 5. Posterior time estimates under fossil calibration strategy A vs. time estimates under strategy B, under the AR clock model.

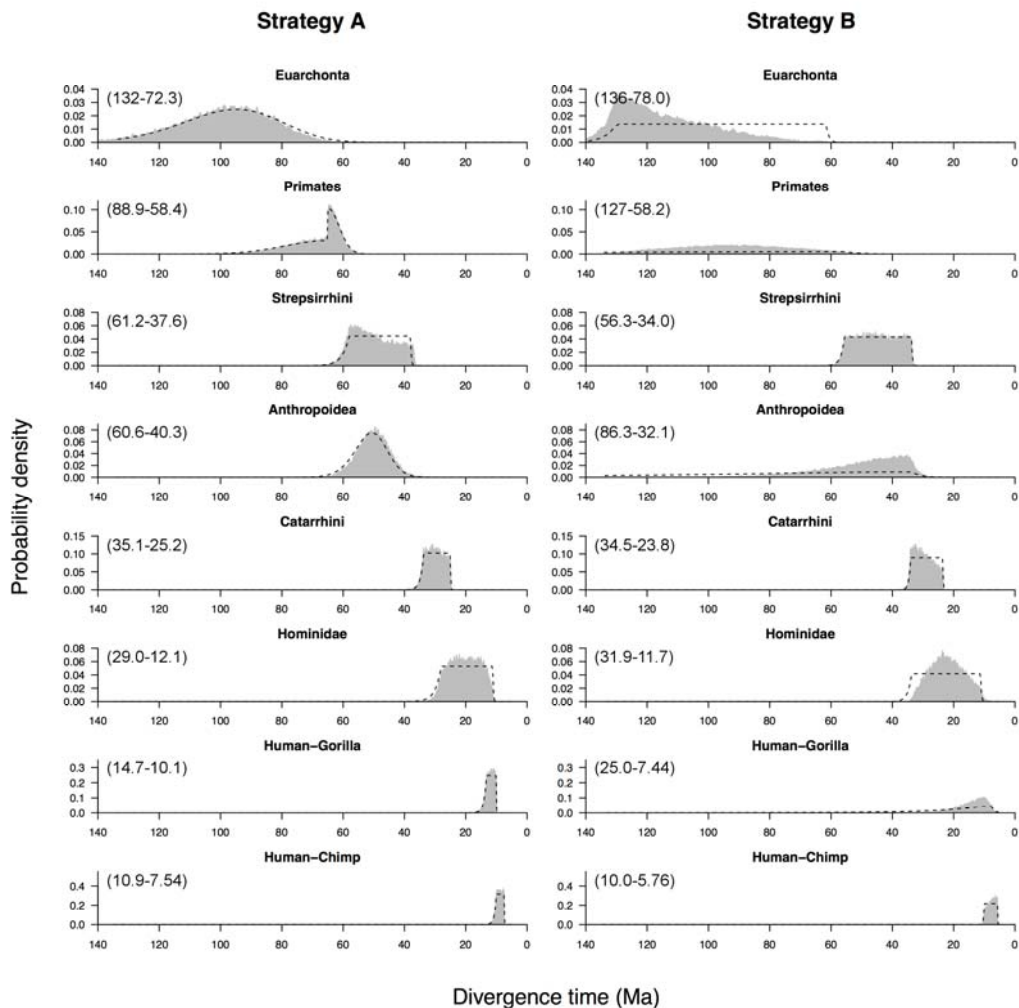


Figure 6. Calibration vs. prior densities for strategies A and B. Numbers in brackets indicate the 95% prior CI. Note that the priors for three Cauchy-based calibrations in strategy B (Primates, Anthropoidea and Human-Gorilla) have heavy tails that extend substantially back in time.

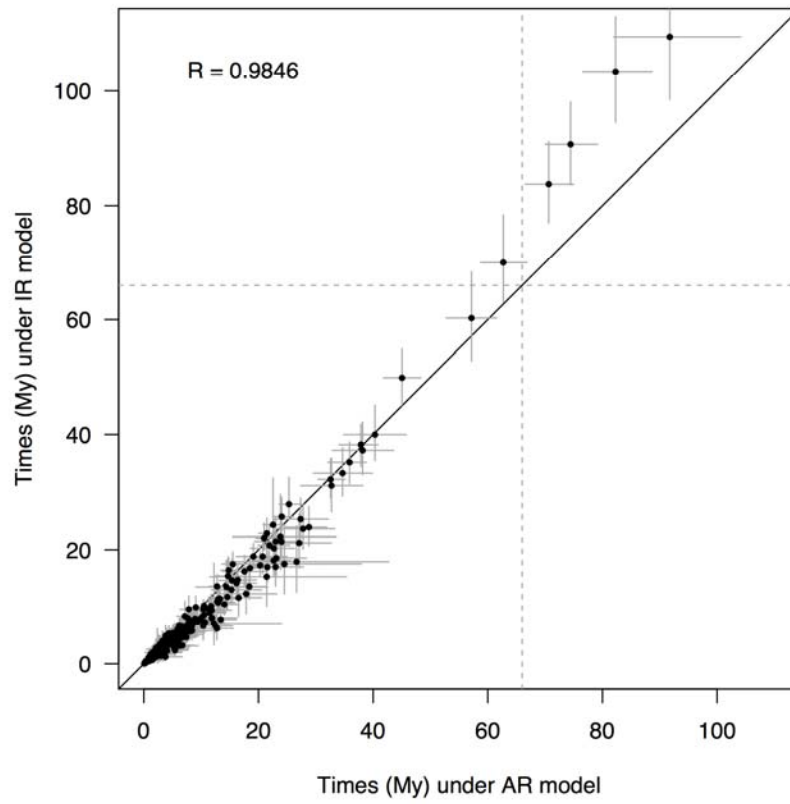


Figure 7. Posterior time estimates under the AR vs. IR clock models, for calibration strategy A.

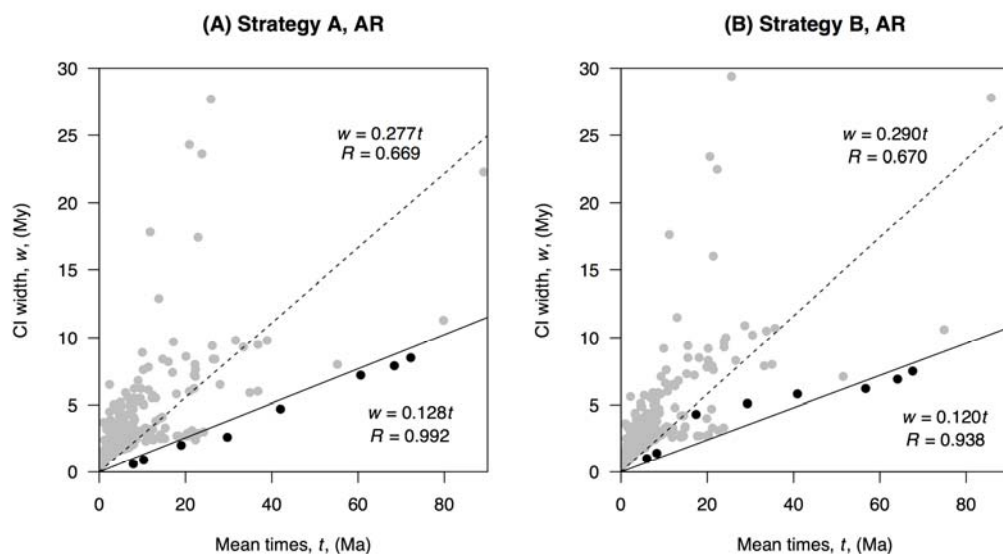


Figure 8. Infinite-sites plot. Posterior CI width is plotted against mean posterior divergence times for (A) analysis under calibration strategy A and AR clock, and (B) analysis under calibration strategy B and AR clock. In both cases, black dots indicate the eight primate nodes shared between the 10-species and 372-species trees, while the grey dots represent the rest of the nodes. Solid line: regression through the origin fitted to the black dots. Dashed line: regression through the origin fitted to all the dots.